Electrocoalescence of Water Droplets in Oil Emulsions: Effect of Electric Fields, Surfactants, and Chemical Demulsifiers

by

Carol Dwaik

A thesis submitted in partial fulfillment of the requirements for the degree of

Master of Science

in

Chemical Engineering

Department of Chemical and Materials Engineering
University of Alberta

Abstract

Stabilization of water-in-oil droplets during bitumen extraction and refining process poses a major challenge in the oil sands industry. These crude oil emulsions are stabilized by rigid films at water droplet-oil interfaces. The salty water remaining in oil causes equipment corrosion, catalyst poisoning in upgrading, lower product quality and extra transportation capacity, all of which immensely increase operation costs.

An effective and clean method used for water removal is the integration of electric fields with chemical demulsifiers. Past studies proved that coalescence of water droplets under external electric field is significantly enhanced through increasing electric field strength up to critical voltages in various setups. However, more in-depth experimental tests are needed to understand fundamental interactions using model emulsions (i.e., droplet-droplet, thin films, oil phases), and to link to industry applications. This research investigates the use of electric fields in chemical and physical variations to combat stable emulsions in bitumen extraction processes.

To understand the various phenomena that occur in water-in-oil emulsions, a setup of water-water droplets in oil is tested using a high voltage-modified Thin Film Draining Apparatus (TFDA). The experiments are split into two main sections, one investigates the effect of electric field variables while the other considers the effect of chemical and physical variations of emulsion systems. To elaborate, electric field variables include the application method of electric fields, such as ramp speed and field strengths. The results show that faster ramp speed leads to shorter coalescence time, and high field strengths cause unwanted droplet stringing (i.e., further emulsification); it is therefore crucial to evaluate these variables. Alternatively, chemical and physical properties of the emulsion systems were investigated, including the effect of type and

concentration of demulsifiers, droplet size, and droplet overlap on electrocoalescence of water droplets in oil emulsions.

The results of these experiments allow us to establish correlations among electric field and physical/chemical properties to gain a fundamental understanding in enhancing coalescence and demulsification, thus leading to more efficient phase separation.

Supplemental material related to this thesis is available at https://era.library.ualberta.ca/collections/7p88ck40x

Acknowledgements

I would like to express my sincerest gratitude to my co-supervisors, Dr. Zhenghe Xu and Dr. Qingxia Liu for granting me the opportunity to participate in this research project. They have acted as my mentors, while supporting and challenging me to be a diligent researcher. For that, I will always remember to ask questions and seek answers whenever possible.

Thank you to Mr. James Skwarok, Ms. Jie Ru, and Ms. Lisa Carreiro for their consistent efforts to maintain our organized protocols and safe lab spaces. I am greatly appreciative of their support, professionalism, patience, and kindness. Thank you to Mr. Walter Boddez, Mr. Les Dean, and Mr. Herb Green from the Chemical and Materials Engineering Shop for their diligence in creating multiple elements in the experimental setup. I extend my sincerest thanks to my fellow research group members that assisted me as well, including Dr. Rogerio Manica, Mingda Li, and Ye Zhang.

To Dr. Vinay Prasad and Dr. Ken Cadien for advising me through various aspects of my program, thank you for the support and guidance. To Professor Johan Sjoblom, thank you for the valuable discussions.

Finally, I would like to thank our research group industry partners as well as the Norweigan Research Council under the Joint Industry Project (JIP) of Electrocoalescence for their financial support and project collaboration efforts.

Table of Contents

List of Tables

List of Figures

Chapter 1 Introduction

1.1. Background and purpose

The presence of dispersed water droplets in crude oil is widely common and highly undesirable occurrence in petroleum industry, which results in corrosion of the process equipment, possible catalyst-poisoning in upgrading, and extra transportation cost owing to increased volume as well as increased viscosity [1]. Asphaltenes work to stabilize emulsion films, complicating the phase separation of water from crude oil mixtures [2]. The emulsified water is in the form of micrometer sized droplets which carry dissolved salts that add to the corrosion problems in downstream refinery, equipment, and transporting pipelines. The production of high quality crude or heavy oil requires cost efficient methods for removal of emulsified water and is in high demand by oil and gas industries; hence, the study of emulsion properties is an important area for research.

A method to break water-in-oil (W/O) emulsions is through coalescence, the process where two droplets merge to form a larger droplet. When two droplets approach one another, their interface is separated by a thin film of oil, which works to maintain emulsion stability; coalescence requires rupturing of this interfacial film. Coalescence has proven to be an important method for demulsification or dewatering crude oil in the petroleum industry and is dependent on many factors including the collision rate (or mixing), interfacial tension, interfacial layer rheology and rigidity, and attractive forces. There are various methods available to promote the coalescence of water in oil emulsions, including the use of chemical demulsifiers, electrocoalescers, high heating treatments, and centrifugation. Electrocoalescers utilize electric fields to trigger coalescence among water droplets in oil emulsions, hence assisting in phase separation to break W/O emulsions. Integrating electric fields have proven to be an effective and clean method for water removal, which is why electrocoalescence is a popular field of research. Under electric fields,

water droplets are shown to be more readily deformed and elongated, which promotes drop-drop contact, enhancing coalescence rates. However, a field that has not been fully explored is the combination of electrocoalescence with the addition of chemical demulsifiers. There are also many gaps that do not evaluate other properties of electric fields, and how they may influence droplet behavior in a W/O emulsion. Hence, it is critical to look into different variables that may affect droplet behavior and combine such variables with the addition of other chemicals, including demulsifiers and surfactants, in order to gain a better understanding of the coalescence processes occurring.

1.2. Research objectives and thesis outline

This research investigates the use of electric fields under chemical and physical conditions to combat stable emulsions in bitumen extraction processes, thus leading to more efficient phase separation. Objectives of this work include:

1. To determine mechanisms of enhanced demulsification through studying electrical, chemical, and physical variables.
2. To study the impact of combining chemical demulsifiers with electrical fields on coalescence processes.
3. To understand stabilization mechanisms of water-in-oil emulsions by studying properties of interfacial film.

The present thesis contains five chapters, including the introduction in Chapter 1.

Chapter 2 provides a literature review that covers the fundamentals of W/O emulsions, the process of coalescence and electrocoalescence, and electric field effects on droplets, as well as other areas of research that will be explored in experimental results. An overview of surfactants, asphaltenes, demulsifiers, and previous experimental methods will be discussed.

Chapter 3 includes the materials used in this work, as well as experimental methods, equipment, processes, and setup.

Chapter 4 contains results and findings, as well as discussion pertaining to the study.

Chapter 5 summarizes the work done and includes future research areas to be explored.

Chapter 2 Literature Review

2.1. Water-in-oil emulsions

Colloids are dispersions of two different mediums, where the first is a continuous medium and the second are particles dispersed within the first phase [3]. Water-in-oil emulsions are a type of colloidal dispersion, where water is the dispersed phase (in droplet form) and the oil is the continuous phase [3]. Stable water droplets dispersed in crude oil emulsions during processing stages is a complex and unfavorable consequence in bitumen extraction. Crude oil naturally contains various volumes of water, which can vary with aging time as well [1]; this volume may vary from below 1% to over 70% of the total produced volume, with droplets sizes at or less than 5 μm in diameter [3]. As a result, the presence of water may cause equipment corrosion, catalyst poisoning, and increased transportation volume, all of which increase processing and handling costs for petroleum industries [4]. In the oil sands industry, water may be emulsified into the oil phase during slurry preparation as well as during hydrotransport, however, a major contributor alongside stable water droplets themselves is the salt that is carried within the emulsion, which cause serious corrosion problems in pipelines and refineries [3]. Other applications of applied electric fields on fluid interfaces also include electrospraying [5], [6] and mixing [7], while dispersed water droplets in organic liquids (W/O emulsions) specifically are encountered in chemical and biochemical industries [8], [9], [10], including food, cosmetics, paper, paint, etc. [11]. Figure 1 outlines many of the factors and stages in electrically induced separation of W/O emulsions.

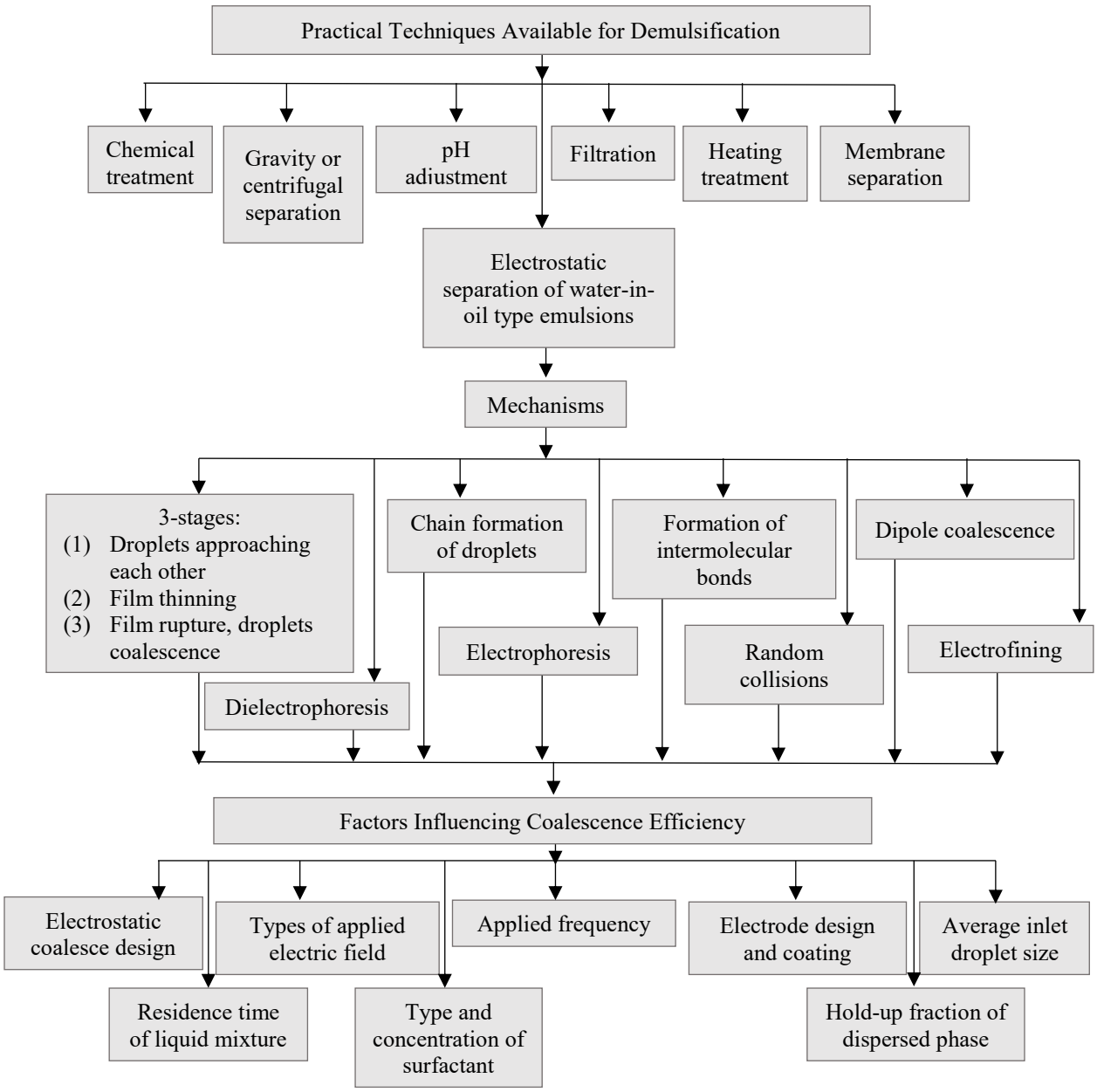

Figure 1. Mechanisms and factors influencing the coalescence efficiency of electrostatic separation of water-in-oil type dispersions. [12]

Emulsions in the petroleum industry are very difficult to break and overcome, indicating that stabilization mechanisms are in place, which slow down phase separation [3]. More specifically, water in crude oil (W/CO) emulsions are usually very stable and difficult to eliminate. It is difficult

to declare exactly how these emulsions were created, as some may already be present in the oil reservoir, carrying water as they migrate [3]. However, it was discovered that most emulsions are likely formed as the oil flows into the well bore or turbulent flow on chokes and valves on centrifugal pump impellers [3]. Crude oil emulsions contain asphaltenes, inorganic particles, or other natural surfactants [13] that form rigid interfacial films on water droplet surfaces [14], working to stabilize water-in-oil emulsions by preventing droplet-droplet coalescence, resulting in difficulties with phase separation. In other industries however, such as food industries, maintaining a stable emulsion is a desirable outcome, therefore the coalescence phenomenon is prevented in these circumstances [15]. There are several techniques used to obtain dehydration, the removal of water and salt present in crude oil and petroleum extractions, including chemical demulsification, pH adjustment, gravity or centrifugal settling, filtration and heating treatments [16]. However, these processes become quite time consuming due to more stable emulsions and are not always cost effective as industries spend millions of dollars on either preventing or breaking down W/CO emulsions [3]. Electrocoalescence (or electrostatic demulsification) is a technique used to combat these issues [17] and will be discussed in detail further on in Section 2.4.

Solid particles at the interface of droplets do not lower interfacial tension, they work to lower the free energy of the system, hence resulting in the same outcome of stabilized emulsions as illustrated in the following figures. Many solid light particles stabilize petroleum emulsions, including asphaltene aggregates, clays, coal particles, and organic or inorganic materials insoluble in the continuous oil phase [3].

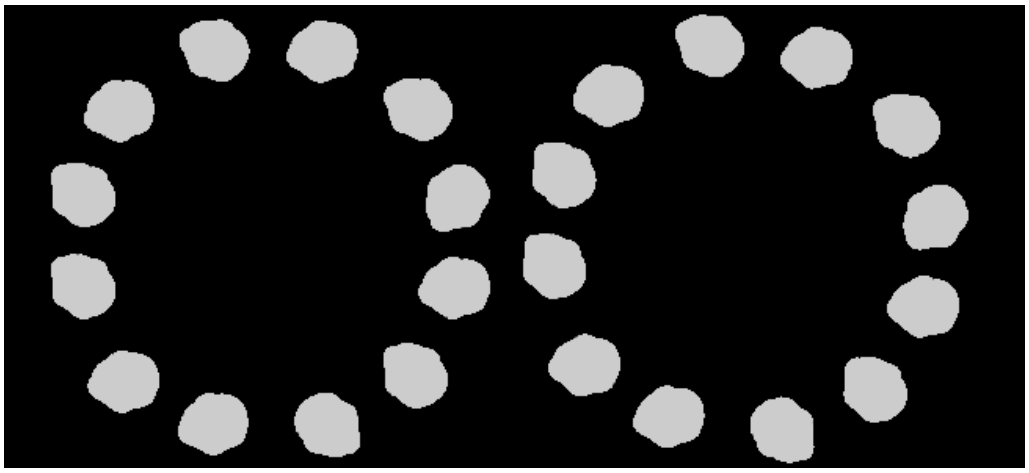

Figure 2. Steric stabilization barrier formed by solid particles. [3]

This schematic illustrates particle layers at the drop surface providing steric (i.e., mechanical) hindrance to droplet coalescence, stabilizing emulsions for years [18], [19]. Asphaltenes are heavy, polar, and surface-active component of crude oils (however this is not always the case in all asphaltene molecules) [3], hence, they are the main contributors for W/CO emulsion stability in the petroleum industry; their characteristics are discussed more thoroughly in the upcoming Section 2.3.

2.1.1. Interfacial tension

The term interfacial tension (IFT) is used in a liquid-liquid or solid-liquid system to describe the excess energy associated with the existence of the interfacial boundary, while surface tension is reserved for a gas-liquid interface [3]. Its' role in droplets with an interface is made clear using equation (1) below:

$$dW = \gamma dS = \gamma 2\pi r dr \qquad (1)$$

Where dr is the change in radius and $2\pi r dr$ is the change in surface area (or $4\pi r^2 dr$ for volume). Due to the conservation of energy, dW is the change in work or energy of the droplet, which must be equal to the right-hand side of the equation. The interfacial tension (γ) then is a

proportionality factor with a dimension of energy per unit area which works to maintain a proportionate increase or decrease of work/energy with the increase or decrease of surface area (or volume) of a droplet [3]. Another critical evaluation, the Young-Laplace equation, describes the pressure difference across any curved interface as a result of the work performed against a pressure difference between the inside and outside of a droplet. The simplified derivation is described below in equations (2) to (5):

$$dW = \Delta p dV \tag{2}$$

Substituting the left-hand side of the equation with the IFT relation in equation (1) and the right-hand side with the change in volume, we get:

$$\gamma 2\pi r dr = \Delta p 4\pi r^2 dr \tag{3}$$

$$\Delta p = 2\gamma / r \tag{4}$$

$$\Delta p = \gamma \left(\frac{1}{r_1} + \frac{1}{r_2}\right) \tag{5}$$

Where r_1 and r_2 are the two principal radii of the droplet's curvature. A further application of the Young-Laplace problem is evaluated and described in the upcoming Section 2.5.

The thin film separating stable emulsion droplets is the part of the continuous phase of the liquid, thinning out as droplet approach until the surface forces between the droplets begin to interact with one another [3]. Including a surface-active substance or surfactant at the oil-water interface will work to lower the interfacial tension between droplets, which in turn will further stabilize them by preventing coalescence, promoting dispersion, and maintaining an emulsion [20], [21]. Experimental methods for measuring surface and interfacial tension include the capillary rise method, maximum bubble pressure method, Wilhelmy plate method, Du Noüy ring method, drop shape method, spinning drop (or spinning bubble) method, drop weight (or volume method, and various micropipette methods [3]. The drop shape method (or pendant drop) is commonly used to

measure IFT and can be done so by capturing various photographs of a droplet profile, calculating the shape variation under a specific change, then evaluating the IFT or surface tension by fitting the recorded drop shape to the solution of the Young-Laplace problem.

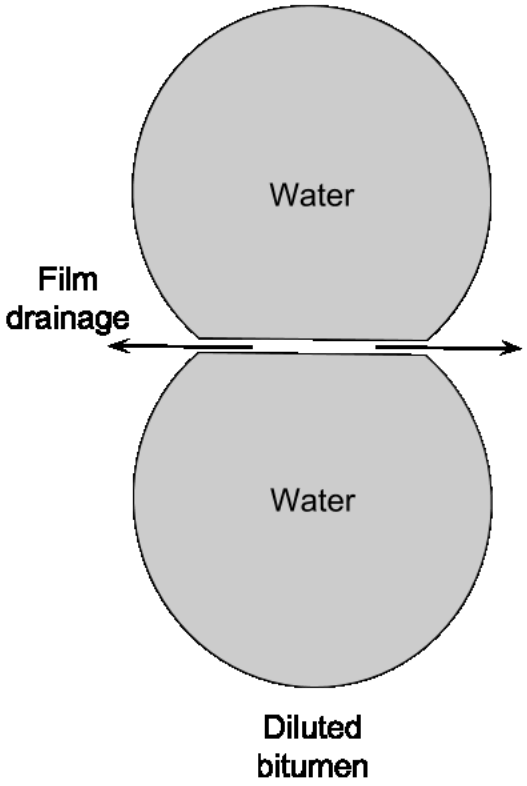

Figure 3. Thin liquid film in emulsion. [3]

2.2. Surfactants

In order to form experimental water-in-oil emulsions, the oil phase must be modelled using specific materials to best imitate the interactions that would occur in an industry setting. Two droplets of the same phase (i.e., water) in a pure oil solvent require a surfactant to stabilize them, otherwise, they would coalesce immediately upon coming into contact [22]. Therefore, in order to model a stable emulsion, an emulsifier or emulsifying agent may be utilized [3]. The term surfactant is derived from the words “surface active agent”, referring to chemicals that are active at water-air or water-oil interfaces; surfactants may be utilized as an emulsifier [3]. They are

composed of two parts, a hydrophilic (water-loving) polar head and a hydrophobic/lipophilic (water-hating) hydrocarbon tail; classifying surfactants as amphiphilic due to their affinity for water and oil, as they are partly soluble in both [3].

Surfactants play an important role in many industries and processes, including wetting, detergency, washing, and foaming [3]. The active parts of the molecules determine the surfactant classification type as either anionic, cationic, and non-ionic [3]. A common surfactant utilized in previous research and experimentation are Span surfactants, as they are effective in reducing interfacial tension [23] and result in increased viscoelasticity observed in the water droplets [21]. Viscoelastic interfaces enhance emulsion stability by increasing the magnitude of steric hindrance and by delaying the rate of liquid drainage between coalescing emulsion droplets [19].

Reduction in interfacial tension causes a degree of stability to the oil-water interface, working to prevent immediate droplet coalescence in experimentation and hence enabling a stable emulsion by reducing phase separation [24]. It has been reported however that the surface active properties of a surfactant contribute more to the strength of the interfacial film (and hence emulsion stability) as compared to its effect of interfacial tension over longer periods of time [24], [25], [26].

Non-ionic microemulsion systems are much less sensitive to electrolytes than are ionic systems, unlike system temperature, which is an important variable in studying microemulsion properties [25]. Even with this, it was discovered that the interfacial elasticities of Span 80 decreased with increasing sodium chloride concentration in the aqueous phase [27]. Span 80 is a nonionic surfactant (synonym: sorbitane monooleate, sorbitan oleate), with fatty acid composition of oleic acid (C18:1) $\leq$ 60%; balance primarily linoleic (C18:2), linolenic (C18:3) and palmitic (C16:0) acids [28]. A common formula for Span surfactants is R-$(OCH_2CH_2)_n$OH [3]. The occurrence of decreased interfacial elasticity with increasing salt concentration is due to the

sodium and calcium ions being hydrated over the surfactant molecules, resulting in a "salting out" phenomena of the surfactant molecules, which causes a reduction of water interaction with the surfactant polar head groups present at the water-oil interface [27]. Consequently, this salting out process will result in decreased surfactant interfacial tension and elasticity [21]. The following research data support the necessity for the interfacial absorption of the surfactant head groups with the water phase in order to obtain an increase in interfacial viscoelasticity, due to the hydrophobic interaction between the fatty acid chains [21].

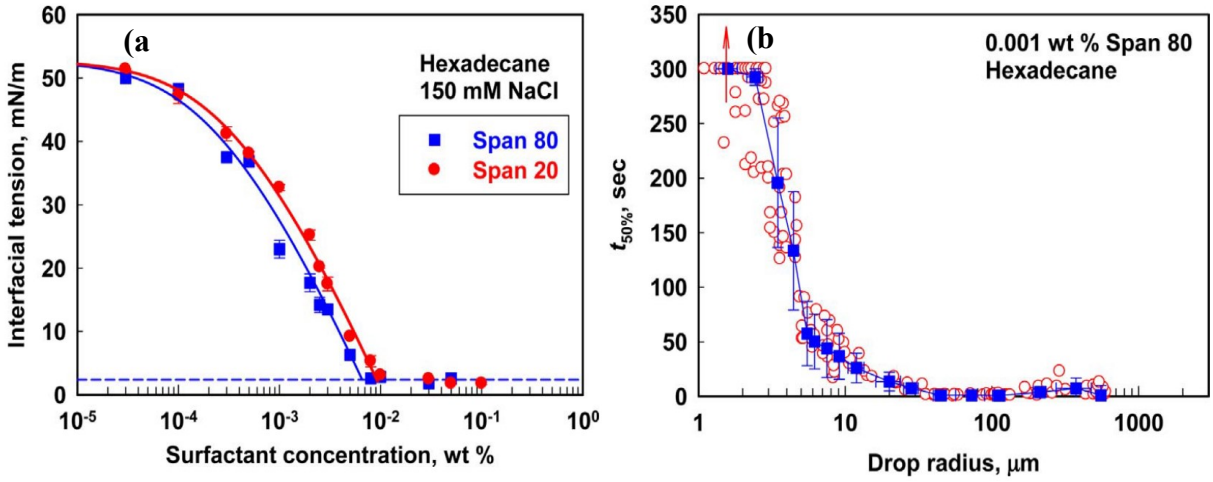

Figure 4. Graphs of (a) water drop interfacial tension under Span surfactant and (b) lifetime of water drops distributed in Span 80 (in hexadecane) solution. [29]

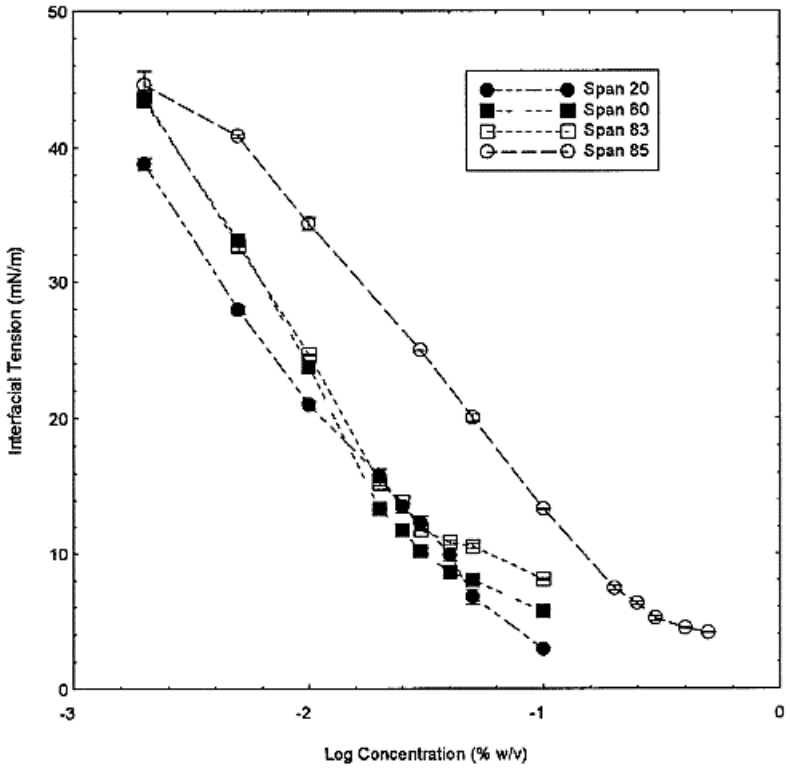

Figure 5. The effect of log bulk concentration on the interfacial tensions of Spans 20, 80, 83, and 85 at the mineral oil/double distilled water interface. [21]

Span 20, 80, 83, and 85 represent different sorbitan surfactants, including sorbitan monolaurate, sorbitan monooleate, sorbitan sesquioleate, and sorbitan trioleate, respectively [21]. These graphs illustrate and confirm the necessity for incorporating a surfactant in order to stabilize a model emulsion for experimentation with high voltage usage. They show a direct correlation between surfactant concentration working to lower interfacial tension in an emulsion system.

A surfactant laden solution in the absence of electric field will prevent coalescence of the aqueous droplets due to the disjoining pressure resulting from the tail-tail interaction between the surfactant molecules on the droplet interfaces [17]. When the electric field is above a critical value for the system, the effect of electric stress overcomes the disjoining pressure between the water droplets, which results in coalescence [17]. The disjoining pressure is the summation of repulsive

and attractive (or van der Waals) stresses. To clarify, the Maxwell stress, which is due to the external electric field, must first deform the droplets against the interfacial tension (IFT) so that the droplets come in contact and then overcome the disjoining pressure for coalescence to occur [30]. In other words, the droplets will coalesce once the applied electrical field voltage is higher than a critical voltage in which the Maxwell or electrical stresses overcome the disjoining pressure [17]. Coalescing separated droplets require that the Maxwell stress first deforms droplets against the interfacial tension to promote drop contact, then must overcome the disjoining pressure for coalescence to occur [17].

2.3. Asphaltenes

Asphaltenes are most appropriately defined as the fraction of crude oil that is insoluble in simple straight-chain alkanes (such as pentane or heptane) but is insoluble in toluene [3]. This definition describes asphaltenes as a solubility class rather than a specific type of chemical with different functional groups due to its variation in molecular mass, composition, functionality, polarity, and many other properties typically used to describe chemical molecules; it is very difficult and ineffective to describe a generalized or typical definition of asphaltene molecules [3].

An elemental analysis on Athabasca asphaltenes are taken as an example to demonstrate the chemistry, specifying that they consist of carbon, hydrogen, nitrogen, oxygen, and Sulphur, with trace amounts of vanadium and nickel and a hydrogen to carbon ratio (H/C) of ~ 1.2 [3]; Table 1 below provides a summary of the weight percent composition of Athabasca asphaltenes, giving an approximation as to which elements make up the bulk of the structures.

Table 1. Elemental composition (wt. %) of Athabasca asphaltenes. [3]

C	H	N	S	O	H/C
79.9	8.3	1.2	7.6	3.2	1.24

Predictably, it is very difficult to estimate the molecular mass of asphaltenes as it is difficult to narrow down the elemental composition of asphaltenes in general as discussed previously. Based on modern analytical chemistry techniques, the molecular mass of asphaltenes is estimated to fall within the range of 400 Da to 1500 Da, averaging around 750 Da; however, vapor pressure osmometry (VPO) and gel permeation chromatography (GPC) estimate much higher values ranging from 3000 Da to 10 000 Da [3]. The conflicting ranges due to various factors within experimental methods themselves (e.g. Uncertainty, method requirements, size, geometry, charge density, etc.), resulting in controversy regarding the most accurate molar mass range for asphaltenes [3].

Asphaltenes vary greatly from surfactants, as they do not have clear hydrophilic polar heads or lipophilic non-polar hydrocarbon tails, thus lacking amphiphilic properties; though, these properties may be contained within the bulk of the asphaltenes, they are not clearly visible. Steric repulsion effects due to the hydrocarbon tails [3] and poor solubility in the parent oil [31], [32] may be the main contributor as to limiting asphaltene aggregate growth or preventing precipitation as a separate phase. There are two commonly used models of the asphaltene molecular structure known as the *archipelago* structure and the *island* (or *like-your-hand*) model, with molecular masses of 2000 Da or greater and 500 Da to 1500 Da, respectively; both models are pictured below in Figure 6 and Figure 7, respectively.

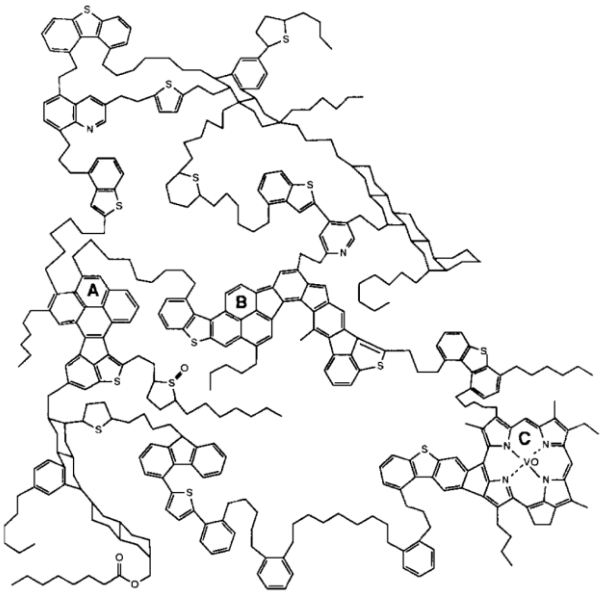

Figure 6. Hypothetical 'archipelago' asphaltene molecular structure with molecular mass around 6200 Da. A, B, and C represent larger aromatic clusters. [3], [33]

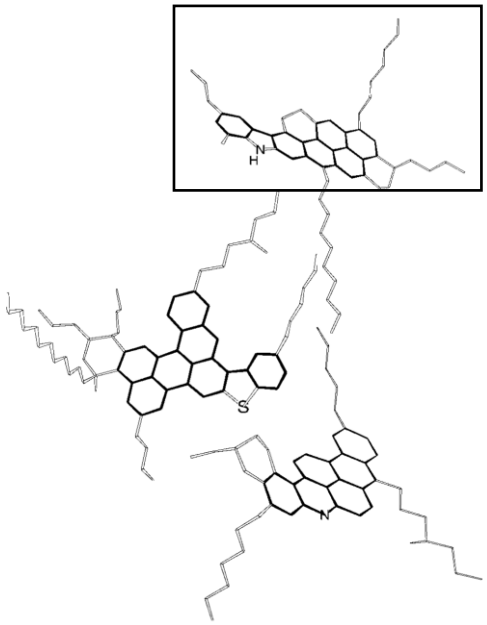

Figure 7. Hypothetical 'island' asphaltene molecular structure with molecular mass around 708 Da for one 'island' component (outlined in box). Aromatic rings are bolded. [3], [34]

2.4. Coalescence and electrocoalescence

The coalescence time, which depends on the liquid bridge evolution, is an important parameter for evaluating the coalescence efficiency [35]. The demulsification efficiency is closely related to the coalescence of droplets in the continuous phase [35]. The coalescence of two droplets in an electric field occurs in three steps: droplet approach, film drainage, film rupture and coalescence (where two droplets become one) [36]. As emulsions are thermodynamically unstable, the system's free energy decreases upon droplet coalescence; however, many emulsions are extremely stable and are difficult to break or separate [3]. Kinetic stabilization explains that although the system is intrinsically unstable, phase separation is slowed down due to the emulsion appearing infinitely stable due to surface forces; hence, in order for coalescence to occur in emulsions, droplets must overcome the repulsive surface forces that maintains the stability of the emulsion [3]. The coalescence process is affected by various factors such as interfacial tension, fluid density, viscosity, pH, and external forces. The degree of difficulty of the drop-drop coalescence is usually measured by the coalescence time, which is defined as the period between the arrival of the drops at the interfacial film and their coalescence [37].

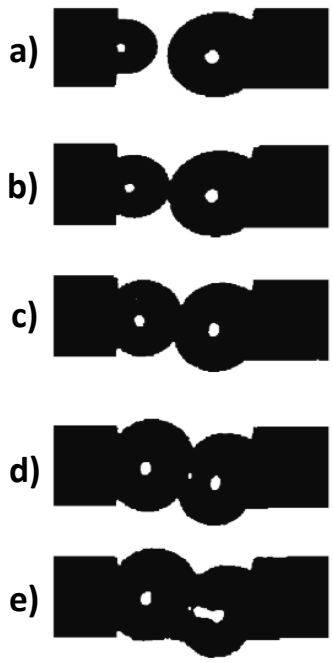

Figure 8. Pair-drop coalescence for a toluene/water system in the absence of an applied electric field, demonstrating a) two drops apart, b) approaching, c) contacting, d) deforming, and e) coalescing. [37]

In the absence of an electric field, a decrease in the interfacial tension has a delaying effect on drop coalescence; lowering the interfacial tension facilitates deformation of the drop surface, as illustrated in Figure 8 [37]. The drops deformed before coalescence occurred, this deformation decreases the pressure applied on the liquid film between the drops, thus delaying the film drainage [37]. Pair-drop coalescence experiments were conducted for aqueous drops with and without applied electric fields, findings claim a decrease in the interfacial tension facilitated the drop coalescence under applied electric fields and could inhibit drop coalescence in the absence of electric field; lowering the interfacial tension enhances drop deformation under external force. Without applied electric fields, such a deformation of the drops increases the resistance to squeezing the liquid film into the interfacial layer and thus inhibiting drop coalescence. However, this research claims that under applied electric fields, lowering interfacial tension facilitates

aqueous-drop coalescence in the organic phase due to the deformation and elongation of the droplets more readily undergoing the Coloumbic force that promotes drop contact and coalescence [37].

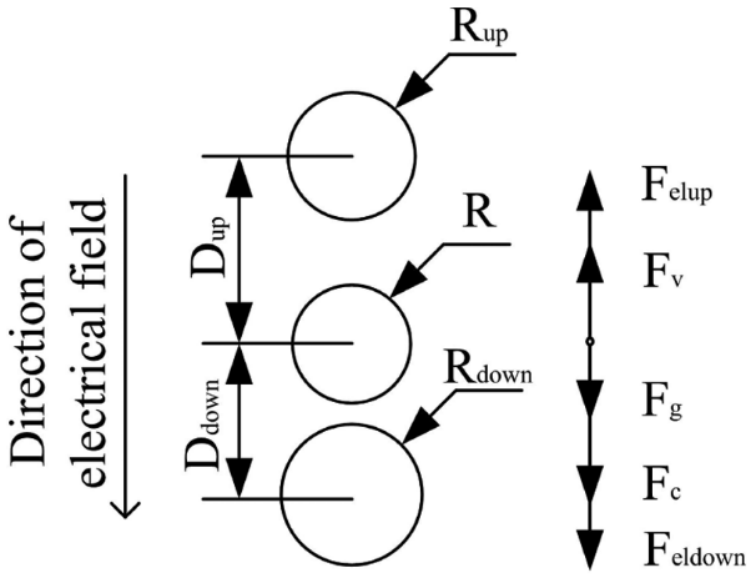

Figure 9. Illustration of the forces acting on droplets in an electric field. [16]

In an electric field, four types of force act on every droplet; these include the electric force (F_{el}) resulting from the effects of the electric field, the Coulomb force (F_C) resulting from the charge of the droplets and the electric field, the viscous force (F_v) resulting from the movement of the droplet and viscosity of the continuous phase, and *the force of gravity* (F_g) resulting from mass and gravitational attraction [16]. Figure 9 illustrates the forces that droplets undergo in an electric field with D representing distance. The electric forces that act between droplets can be further broken down to two parts: the electric force generated because of the existence of the up droplets (F_{elup}) and the electric force generated due to the existence of the down droplets (F_{eldown}) [16]. Droplets in an emulsion, when exposed to an electric field, also experience dipolar attraction which drives the adjacent droplets closer [38].

It is commonly understood that a charged drop in a DC uniform electric field exhibits a motion, direction of which is determined by polarity of the charge; this phenomenon is known as electrophoresis, However, it is important to note that a droplet is not necessarily required to be charged in order be set it the motion in an electric field, or to be deformed by this motion due to its' interactional movement with the electric field. An uncharged droplet experiences a net force and undergoes a translational motion under exposure of an electric field; this particle-field interaction is known as dielectrophoresis (DEP) [39]. Another critical quality of an electric field-based system is whether there is non-uniformity of the applied electric field or non-uniformity of the field due to irregularities of the electrode surface/setup, which also results in dielectrophoretic behavior of the droplet [16,17]. In a multi-drop system, where a large number of drops of one phase are dispersed in another fluid, magnitude of the electric field between two neighboring drops is always higher than that of the applied field [18]; resulting in dielectrophoresis which contributes to the drop–drop interaction [39]. Therefore, dielectrophoretic mobility assists and may even trigger the segregation of droplets in the high electric field region helping to reduce the inter-drop separation distance and in turn increases the probability of the drop–drop contact [40].

Lastly, another important variable mentioned in literature which affects the rate of coalescence is the ionic strength of the aqueous phase in W/O emulsions, that is, the concentration of charged ions contained in a solution. It is shown that for aqueous drops, a higher ionic strength results in a faster coalescence in the absence of an electric field, and a more rapid decrease in the coalescence time with an increase in the applied voltage [37]. This can be explained by an electrical double layer, the charge on the surface and the charge in the solution or bulk forming a system of charges [3], existing at the inner surface of the aqueous drop and causing resistance to drop deformation.

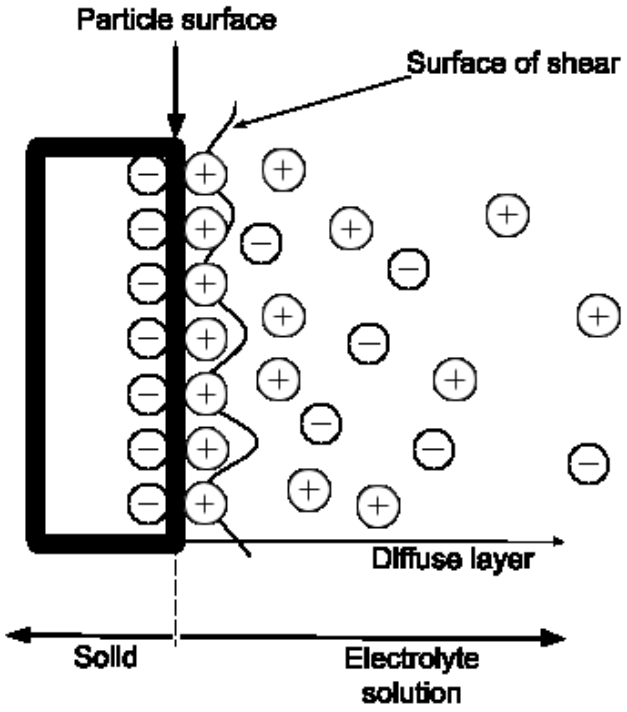

Figure 10. Electric double layer resulting from distribution of charge-carrying ions in the vicinity of a charged interface. [3]

It was observed that in the absence of an electric field, there is a decrease in coalescence time and increase in interfacial tension due to the EDL causing resistance to drop deformation, which makes the aqueous drops more rigid [37]. However, in the presence of an electric field, the aqueous salted drop and the surface of its homophase are polarized under the electric field resulting in an attractive Coulombic force that enhances the drop interface coalescence [37]. Higher conductivity facilitates the surface circulation in the aqueous droplet, which promotes the removal of the organic film from the space between the drop and the interface, also enhancing coalescence [37]. This is shown in Figure 11 through a graph comparing a water phase with and without the addition of sodium chloride. It is important to note here that different forces are more dominant in an electric field as compared to solely relying on interfacial tension such as in the absence of an electric field.

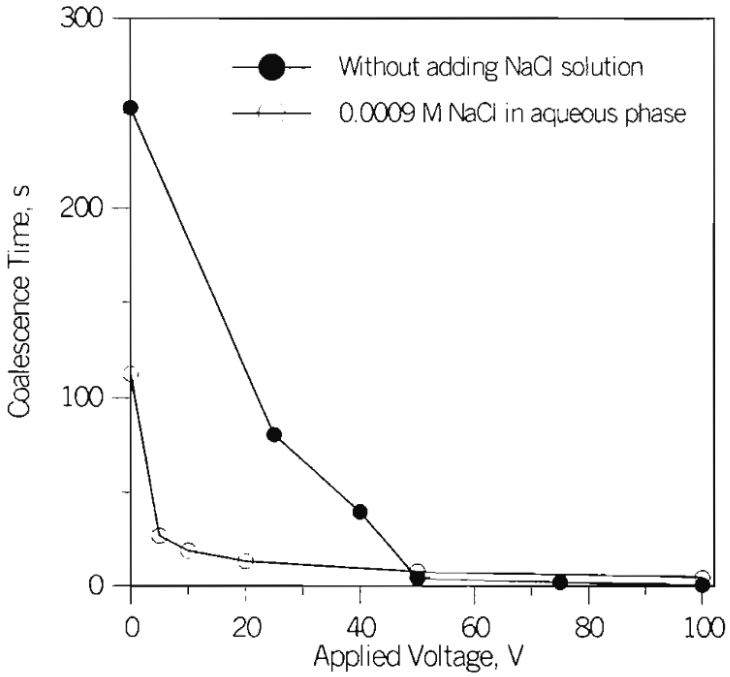

Figure 11. Effect of ionic strength of aqueous drop-organic interface under an electric field. [37]

It is also well-known that the existence of ionic species in emulsions enhances the heating efficiency of the mixture [14]; heating treatments have been previously shown to reduce demulsification times [41] and are commonly used in industries to remove water droplets from a continuous oil phase [42].

2.5. Droplet size and shape in electric fields

An important factor that influences the rate of coalescence is the size of the droplets, which plays an important role in affecting the critical electric field strength under which the drops are coalesced. The critical electric field varies for different size water droplets, generally, the critical electric field strength of larger drops is found to be lower than that of smaller drops [43]. We can refer to equations (7) - (9) as to explain the behavior of larger droplets requiring a higher critical electric field strength [44].

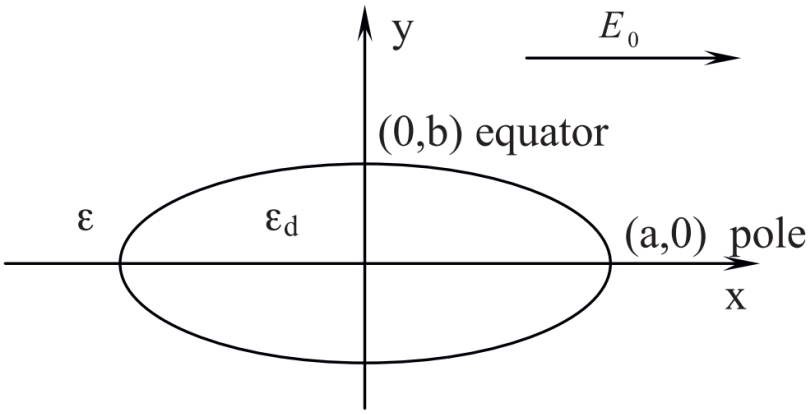

Figure 12. Water drop deformation in an electric field. [44]

In the absence of an electric field, the shape of the droplet will remain spherical due to the interfacial tension (γ) as the surface tension forces (γ/b^2) are greater than that of the body ($\Delta\rho g$) [44]. However, a charged drop can lose its shape stability once the system reaches a certain threshold value of charge [45], known as the critical electric field strength, E_c. Equation (6) gives the Young-Laplace equation which describes the pressure difference across the interface of a drop with radius (r_0).

$$\Delta P = \gamma\left(\frac{1}{r_1}+\frac{1}{r_2}\right) = 2\frac{\gamma}{r_0} = P'_{drop} \qquad (6)$$

This pressure difference is called the capillary pressure in an emulsion with two immiscible liquids, such as oil and water. As the radius of a droplet increases, the pressure difference decreases, easily deforming the droplet. As a result of this, the interfacial tension decreases to equilibrate the relation, increasing the difficulty for the droplet to coalesce.

It is already well known that a droplet's shape and size is deformed under an electric field, such an example is demonstrated in Figure 13.

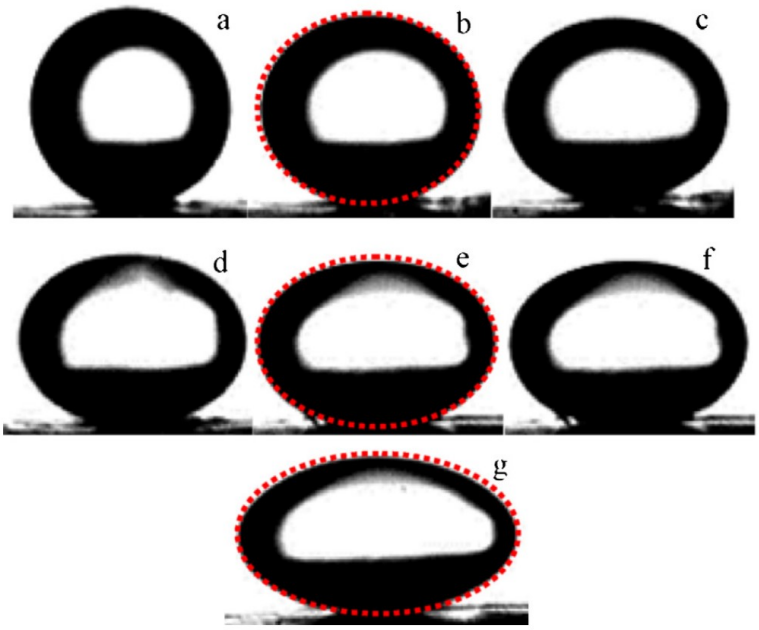

Figure 13. Elongation of a water drop with increasing electric field. Initial drop radius r_0 =267μm. Applied electric field [kV/cm]: (a) 0, (b) 8.9, (c) 10, (d) 11.1, (e) 11.6, (f) 12.3, (g) 12.7. The dashed red lines are perfect ellipses. [44]

Equation (7) gives the pressure equilibrium at the droplet equator and the poles respectively, where a and b (introduced in Figure 12) are the spheroid's semi-axis, Δp is the pressure difference across the droplet interface due to interfacial tension and electrostatic pressure ($1/2\varepsilon E^2$), E is the value of the electric field, ε_0 is the permittivity of the drop and ε is the permittivity of the bulk phase. With this information, the two pressure differences on the spheroid may be balanced so that $\Delta P_{pole} = \Delta P_{equator}$, we obtain the following:

$$E_0\sqrt{\frac{2r_0\varepsilon_0}{\gamma}} = 2\cdot\left(\frac{b}{a}\right)^{\frac{4}{3}}\left(2-\frac{b}{a}-\left(\frac{b}{a}\right)^3\right)^{\frac{1}{2}} f(e) \qquad (7)$$

where

$$f(e) = \frac{1}{2}e^{-3}\,ln\left(\frac{1+e}{1-e}\right) - e^{-2} \qquad (8)$$

The left-hand side of equation (7) is the square root of the capillary pressure as demonstrated in equation (6) and the electrostatic pressure. The right-hand side is the geometric function of the spheroid's semi axis a and b, while $f(e)$ is a function of the eccentricity of the drop due to the applied uniform electric field (E_0). Berg et al. demonstrates that these derivations result in droplet elongation increasing with the electric field strength up until it reaches a stability ratio of $a/b \cong 1.9$; the electrostatic pressure exceeds the capillary pressure above this value resulting in the drop bursting or breaking up. As a result, equation (9) is derived, where E_c is the critical electric field value at which the droplet breaks up.

$$E_c = 0.648\sqrt{\frac{\gamma}{2\varepsilon r_0}} \qquad (9)$$

Figure 14 below shows the theoretical drop elongation of water droplets as a function of the applied electric field, with values of $\varepsilon_0/\varepsilon$ plotted [44].

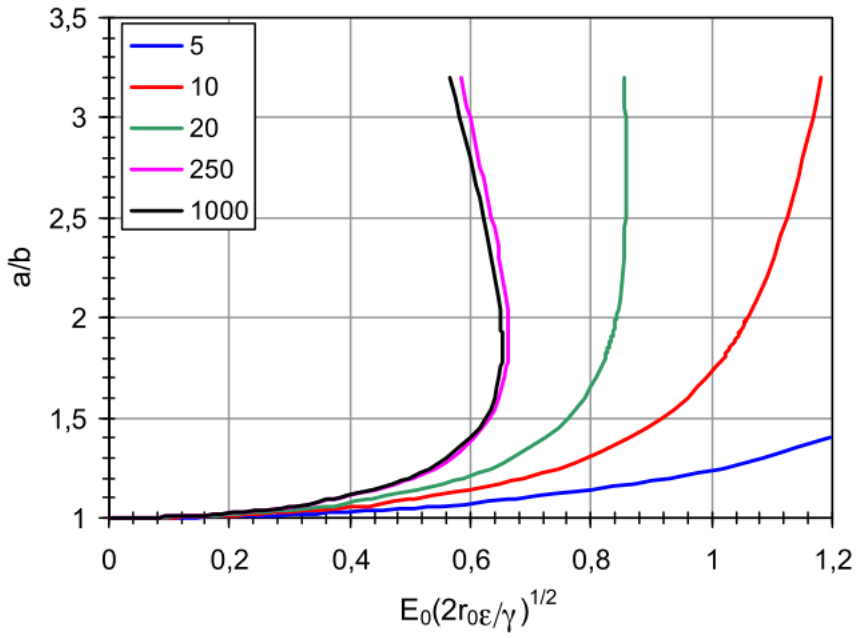

Figure 14. Theoretical elongation of a water droplet as a function of the applied electric field and permittivity ratio. [44]

Another finding explains that once the droplets come into contact, smaller droplets exhibit a faster merging rate than larger ones; this is due to smaller droplets having a larger ratio of the surface water molecules, which possess greater mobility than the interior water molecules [46]. This allows for greater surface activity among smaller droplets. As a result, the merging occurs after the two smaller droplets come into contact within a shorter period of time. One source supports claims that the value of the critical electric field for the onset of drop instability is influenced by the initial drop size [47], which is in fact true according to findings previously explained and derived. It is evident that a larger initial drop will require a lower electric field strength to cause break-up due to its instability [47], however this can have undesirable results as a larger droplet easily splitting will result in further emulsification due to the addition of smaller droplets. It can also complicate coalescence due to the lower interfacial tension that larger droplets display as discussed previously, hence signifying the clear importance of a critical electric field strength that will contribute to coalescence among water droplets without breaking up larger ones.

2.6. Demulsifiers

Compositions of industry demulsifiers are tailored to address site-specific emulsion stabilization mechanisms [3], the efficiency of a demulsifier is determined by the nature of the emulsion and the characteristics of the demulsifier [48], however, these specific properties may not always be known. Industry demulsifiers are a mixture of various chemicals, such that the product can help with the emulsion problem regardless the physicochemical reason for high emulsion stability; the targeted solutions may include promoting droplet coalescence, causing droplet flocculation, or displacing the steric stabilization layer [3]. The stability of W/O emulsions in petroleum systems is due to a stabilization layer on water droplet surfaces forming a skin that is very difficult to disrupt [3]; hence, an effective demulsifier is a surface-active compound that can

adsorb onto the water/oil interface and change its properties such that water droplets aggregate and coalesce [48].

The concentration of added demulsifier in the oil is very important, not only because of economics, but also because of chemical performance [3]. Starting from very low additions, the product quality improves with increasing dosage and then, after passing over the optimum dosage, deteriorates or remains constant [3]. Similar to the strength of electric fields applied to a W/O emulsion, a higher concentration of demulsifiers (or voltage of field) does not always result in the desired outcome which is counterintuitive, as we tend to think that if something is responding well, then more of it would be even better. Addition of a demulsifier, depending on the function, will enhance the rate of coalescence, even in the presence of an electric field. However, there is a demulsifier concentration threshold where once it is reached, the phase separation ceases to improve [49]. Above a limit, a further increase in demulsifier concentration does not speed up the coalescence, and chemical demulsifiers are almost always used in combination with various mechanical and electrical demulsification methods [3].

Chemical companies have developed several families of effective demulsifiers, the results of their performance in emulsions has provided significant economic improvements [3]. Figure 15 below demonstrates trends of the impacts of various chemical demulsifiers on the percentage of water removal in a W/O emulsion, with some demulsifiers working more effectively than others. The trendlines tend to remain constant after a certain concentration of demulsifier added, proving that there is a threshold limit. The inclusion of centrifugation supports the claim that the use of demulsifiers does in fact require an extra force, in this case, mechanical.

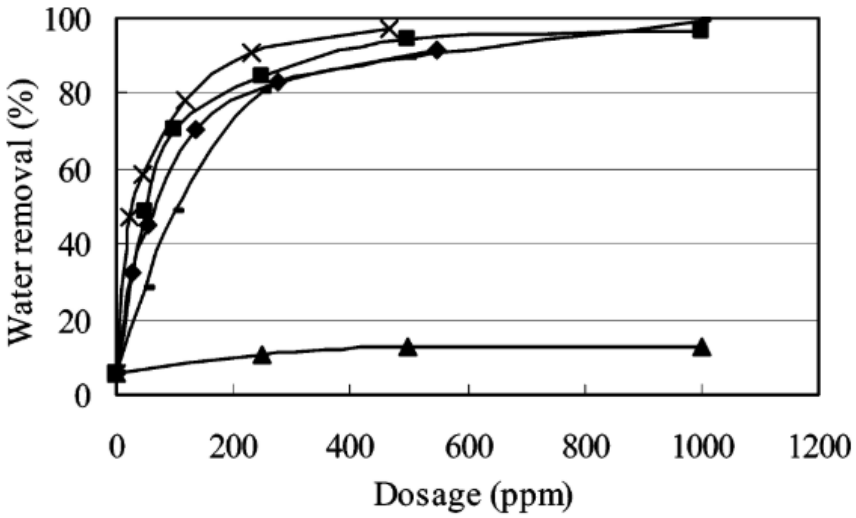

Figure 15. Water removal as a function of demulsifier dosage after centrifugation. [48]

The indigenous surfactants including asphaltenes, resins and some naphthenates are water-insoluble and form a stable thin layer around a droplet [50], making drop–drop coalescence difficult [51], [52]. However, there are only a few studies wherein combined action of chemicals and electric fields [53] in enhancement of the phase separation is investigated.

Nonetheless, combining two methods of phase separation to enhance separation efficiencies has some limitations; therefore, developing new combinations of methods that can break water-in-heavy and/or naturally stable crude oils is essential [49]. An important area that is more recently being investigated is the role of industry chemical demulsifiers in dewatering of heavy crude oil emulsions in the presence of electric fields. The kinetics of asphaltene-stabilized planar films in crude oil emulsions has been extensively studied [2], [54]. Coalescing-type chemicals, also known as interface controller work to promote coalescence of small emulsified droplets in order to result in larger droplets that are easier to separate from and emulsion. Equation (10) yields the total number or droplets (dn_{tot}) as a function of time where a is the distance at which droplets collide and G is the shear rate.

$$\frac{dn_{tot}}{dt} = -\frac{16}{3}a^3 G n_{tot}^2 \qquad (10)$$

In the absence of external forces the thinning rate can be predicted using Stefan–Reynolds equation [55], and the predictions have been proven to be in reasonably good agreement with experimental measurements for crude oil emulsions [2]. Equation (11) below describes the Stefan–Reynolds for the thinning kinetics of a planar film in the absence of an electric field.

$$\frac{dh}{dt} = -\frac{4}{3}\frac{\gamma}{\mu_m}\left(\frac{h}{R}\right)^3 \frac{s^2}{R^2 - s^2} \qquad (11)$$

The film thickness is h, viscosity of medium phase is μ_m, and s is the radius of hole in the porous plate used to form the film in experiments [2]. Modifying the Stefan–Reynolds equation to include the electrostatic effects on the thinning kinetics where the electric field (E_0) is applied across the planar film results in equation (12) below:

$$\frac{dh}{dt} = -\frac{2}{3}\frac{h^3 s^2}{\mu R^4}\left[\epsilon_m E_0^2 + \frac{2\gamma R}{(R^2 - s^2)}\right] \qquad (12)$$

Here ϵ_m is permittivity of oil phase, and the second term on the right-hand side of equation (12) represents the external electric force on the film of the droplet. Since the effects of demulsifier molecules start to appear in the film drainage stage of electrocoalescence and the mechanism of demulsifier-induced destabilization of a thin film is unestablished, the change in interfacial tension is taken into account in the model. Using the governing forces including the resisting lubrication force (F_l) [56], the capillary force (F_c), and the electrostatic force of attraction (F_E) [57], equations (13) to (15) are expressed to derive equation (16).

$$F_l = 16.5\mu_d a \frac{dh}{dt}\sqrt{a/h_0} \qquad (13)$$

$$F_c = 4\pi\gamma\left(a - \sqrt{a^2 - s^2}\right) \qquad (14)$$

$$F_E = -12\pi\epsilon_m E_0^2 \frac{a^6}{(h+2a)^4}(3M - 1) \qquad (15)$$

$$\frac{dh}{dt} = \frac{8\pi\left(\frac{\left(3\epsilon_m E_0^2 a^6 (3M-1)\right)}{(h+2a)^4} + \gamma\left(a - \sqrt{a^2 - s^2}\right)\right)}{16.5\mu_d a\sqrt{a/h_0}} \quad (16)$$

Where a, h, t, h_0, s are radii of the coalescing drops, film thickness, time, initial thickness of the film, and radius of the film which is assumed to be constant during its complete drainage, respectively [49], as illustrated in Figure 16.

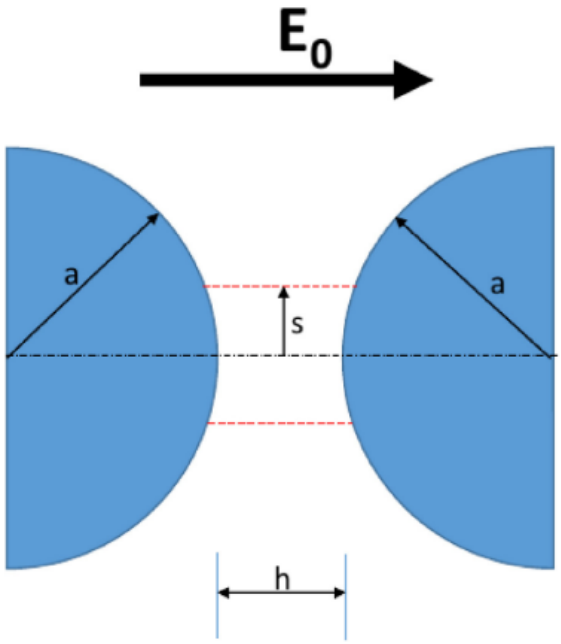

Figure 16. Schematic of two uniform water drops approaching under a constant DC electric field. [49]

M is a derived geometrical coefficient for the radial component of the electrostatic force of attraction [51]. Equation (16) is solved for time evolution from initial film thickness $h_0 = 0.1a$ to film break up of $h_f = \left(\frac{Aa}{8\pi\gamma}\right)^{1/3}$ where A is the Hamaker constant (van der Waals interaction energy constant) of 7×10^{-21}J. This derivation is utilized to effectively calculate the rate of which coalescence may occur between two droplets in a W/O emulsion, showing that the rate of coalescence is governed by physical and electrical properties of the emulsion in addition to the applied electric field [49].

2.7. Experimentation methods

Many experimentation techniques have been utilized in literature in order to evaluate droplet-droplet interactions for W/O emulsions. Two methods are most commonly used, each having advantages and disadvantages. The first method of analyzing W/O emulsions includes visualizing free-moving water droplets immersed in an oil phase. This setup is most representative of an industry emulsion as the water droplets are already pre-dispersed in such a manner. However, a disadvantage is that this experimental method has little control over the behavior of the droplets, and in turn, many variables cannot be studied. This also requires more analyzing techniques for variables such as droplet size distribution (DSD) to ensure uniform droplets within the emulsion. As there are a multitude of droplets, it is increasingly difficult to focus on two droplets up close in order to evaluate coalescence convergence patterns and characteristics of shapes, unless done so with precise video recording techniques and computer programs.

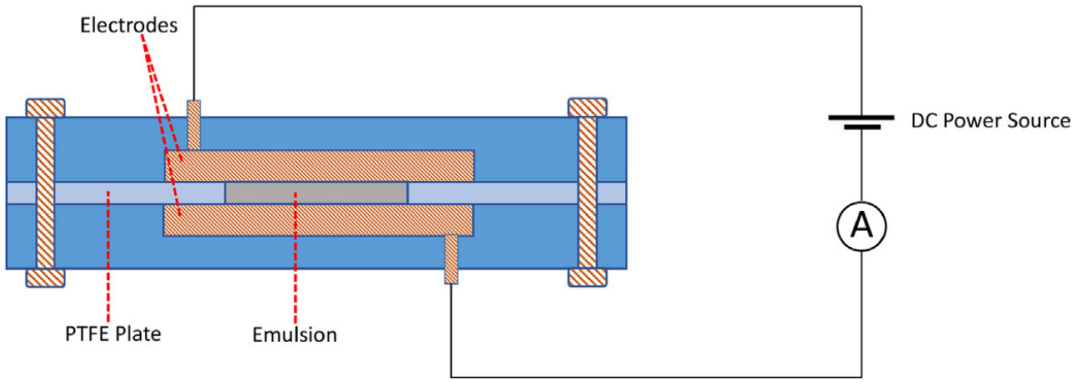

Figure 17. Schematic of electrocoalescence cell to apply an electric field through with a thin emulsion layer of 250µm thickness. [49]

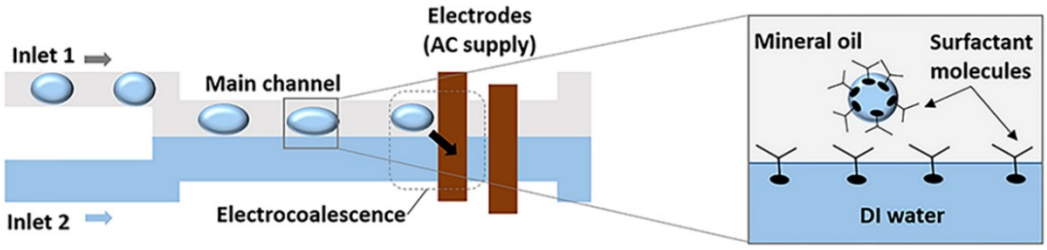

Figure 18. Schematic of microfluidic device for electrocoalescence based droplet demulsification. [17]

Figure 17 and Figure 18 illustrate two experimental methods where water droplets are not anchored in their emulsions, they are free to move and interact with other instances of the water phase. In Figure 17, a very thin W/O emulsion layer is trapped between two electrodes, free flowing inter-droplet interactions are visualized via camera. In Figure 18, droplets are also non-stationary, however, the interaction monitored is that of water droplets with a water layer phase in order to study interfacial properties.

Another common setup includes two anchored (or stationary) water droplets, usually attached to capillary tubes or rods. This allows a much more focused viewpoint to determine shape factors, electrocoalescence, and visualize more thin film characteristics. Otherwise, most experimental setups commonly consist of the same materials, including a high voltage source, a charged electrode, a grounded electrode, a cell to contain the emulsion solution, salted or unsalted water, an oil phase (including some form of surfactant or asphaltenes), and a camera with a light source and monitor to capture the droplets' interactions. Two examples of the stationary droplet setup are illustrated in Figure 19 and Figure 20.

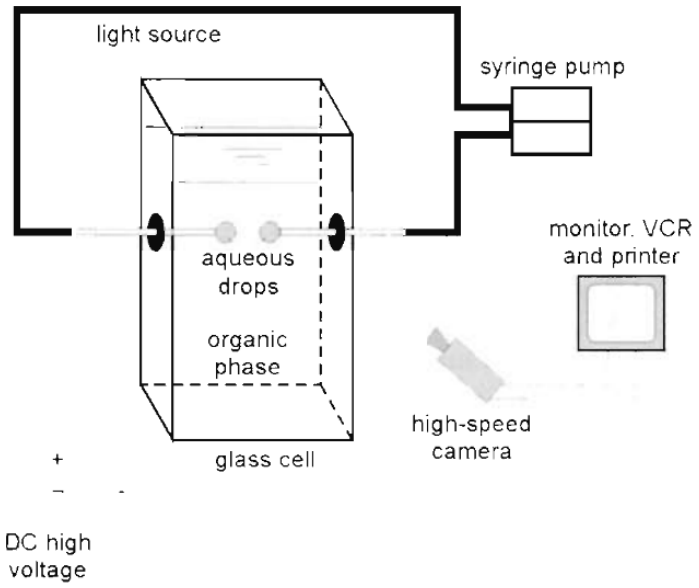

Figure 19. Schematic of experimental apparatus for studying stationary pairs of water drops in an electric field using capillary tubes. [58]

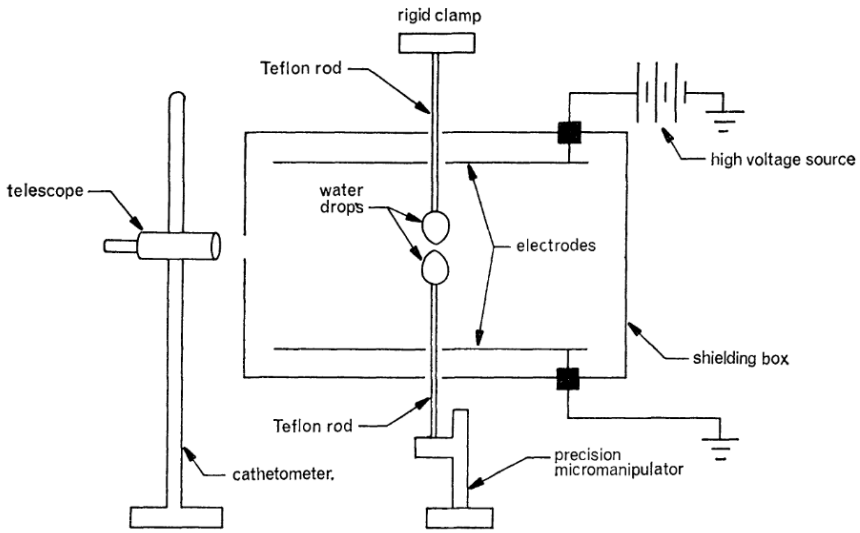

Figure 20. Schematic diagram of experimental apparatus for studying stationary pairs of water drops in an electric field anchored onto rods. [37]

All the above setups are slightly varied; however, they are all sufficient in evaluating and studying surface chemistries and interactions of W/O emulsions under electric fields.

Chapter 3 Materials and Methods

3.1. Materials

ICP solvent, also known as hydrotreated light distillate (petroleum) (≥ 99.9995%), was purchased from Sigma-Aldrich and used as received, with a density of 0.810-0.838 g/ml at 20°C. Span 80 (sorbitan monooleate), was also purchased from Sigma-Aldrich and used as received. Milli-Q deionized water (DI water) was obtained from the laboratory filtration system. Heptane solvent was purchased from Sigma-Aldrich and Toluene was purchased from Fisher Chemical. The extracted asphaltenes used in model oils were provided by Ugelstad Laboratory from Norway.

The three demulsifiers used were delivered for experimentation by Ugelstad Laboratory, received from AkzoNobel and NalcoChampion. These are industry grade demulsifiers, with limited details given due to patents and industrial use. The details that were provided are summarized in Table 3.

3.1.1. Preparation of W/O emulsions

The chemical materials used for these experiments require multiple criteria for each function, this includes the oil phase, the water droplets, surfactant, and demulsifiers. Since these experiments critically test the electrocoalescence of water-in-oil emulsions, i.e., water droplets in an oil phase, it is important to establish stable materials in which the different testing variables may be manipulated and reproducible. The requirements of the water droplets are that they do not coalesce upon impact, but are not altered too much so that they do not resemble water-like properties (in terms of pH, ionic properties, etc…) However, this requirement and most others, are dependent on the properties of the oil phase.

Experiments for both a simple model emulsion and a complex model emulsion are conducted, section 4.2 studies electrocoalescence behavior of water droplets in a *simple model oil* solvent, while results in section 4.3 are obtained by using an asphaltene-based, *complex model oil* with the addition of industry demulsifiers. There are many similarities and differences between solid and surfactant stabilization mechanisms [3], hence it is important to evaluate both types of emulsions.

The simple model emulsion is studied in section 4.2. The oil phase requires the integration of a long chain surfactant in order to modify the surface properties of the water droplets as to prevent immediate coalescence upon droplet-droplet contact. Utilizing a relatively simplistic setup allows the main idea of the research objective be studied, that is, it allows us to hone in on the water droplet and oil phase/surfactant response to electric fields. In this sense, we can gain a fundamental understanding of what is actually being affected by the electric field, and how we can utilize this methodology for future work, in both industrial and academic applications.

The main oil phase used is ICP solvent, a hydrotreated light petroleum distillate typically used with Inductively Coupled Plasma (ICP) technology. It is a reduced toxicity paraffinic oil equivalent to xylene which is also clear and colourless. When testing water droplet interaction in the ICP solvent, the two droplets immediately coalesced upon impact, as predicted. This prevents the experiments from being carried out correctly as there is no stabilization of contacting droplets in order to clearly examine how and where electric fields will act upon the droplets. Span 80 (also known as sorbitane monooleate), is a non-ionic, oleic acid surfactant that was used to combat this issue. Like the ICP oil solvent, it is also colourless and clear with a long chain fatty acid composition, stabilizing the water droplets among impact.

Section 4.3 utilizes the complex model emulsion, with an asphaltene-based oil phase. Previous experimental studies within our research group and literature used the compound C5PeC11 or extracted asphaltenes in combination with a solvent. Solvents usually include toluene, heptane (or heptol—a combination of heptane and toluene), xylene, castor oil, or paraffinic oil. For the complex model oil phase, a maximum quantity of extracted asphaltenes is used in combination with the solvent heptol (a combination of equal amounts of heptane and toluene) which acts to stabilize the water droplets by forming a thin film on the droplets, while also maintaining droplet visualization in the camera view.

Details of the model oil compositions, as well as the water phases and demulsifiers used are provided in Table 2.

Table 2. Summary of model oil emulsions.

		(a) Simple Model Emulsion	**(b) Complex Model Emulsion**
Oil Phase	**Solvent**	Paraffinic oil	Heptol (50/50 heptane + toluene)
	Surfactant	Span 80 (oleic acid)	Extracted asphaltenes
	Concentration	15.5 g/L	0.100 – 0.170 g/L
	Aging Time	none	15 minutes minimum
Water Phase		Milli-Q water	Milli-Q water + 3.5 wt% NaCl (Salted water)
Demulsifiers		N/A	**1.** NalcoChampion A **2.** AkzoNobel A **3.** AkzoNobel B

3.1.2. Chemical demulsifiers

These chemical demulsifiers are used in industry for breaking emulsions; they were obtained from the Ugelstad Laboratory in NTNU for experimentation of behavior under electric fields in the water in model oil emulsions. These demulsifiers are under the ownership of Nalco Champion and AkzoNobel industries, hence their exact composition and properties are limited. They have provided key characteristics summarized in Table 3, which are further explained below.

Table 3. Summary of chemical demulsifiers.

Company	Name	Chemistry/Function	RSN	MW
Nalco Champion	A	Amine alkoxylate/drier	6.9	High
AkzoNobel	A	Fatty acid alkoxylate ester	9.5	n/a
AkzoNobel	B	Fatty acid alkoxylate ester	6.1	n/a

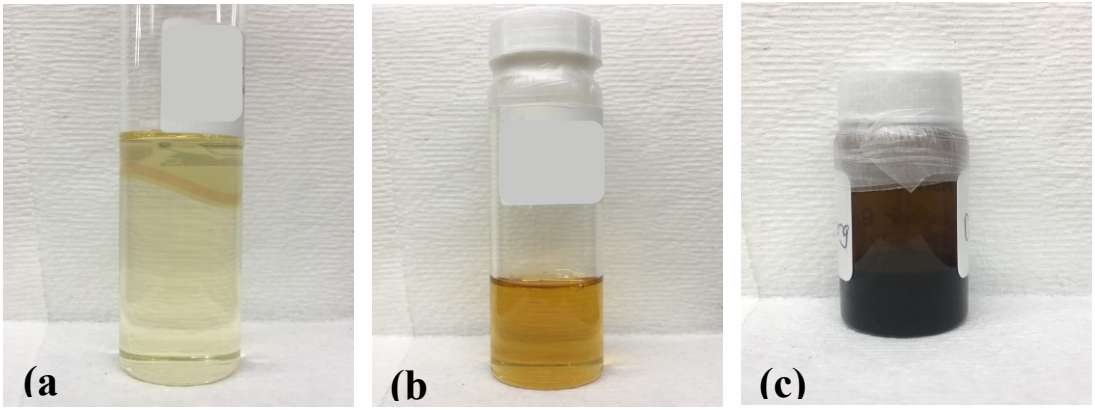

Figure 21. Chemical demulsifiers used in experiments (a) Nalco Champion A (b) AkzoNobel A (c) AkzoNobel B.

3.2. Equipment

The induction timer, known as a Thin Film Draining Apparatus (TFDA), is the main method of measurements used for the experiments. It is a home-built laboratory machine which has been

used for the purpose of measuring coalescence time, thin film drainage, bubble/droplet surface attachment, and studying droplet-droplet/droplet-bubble/bubble-bubble interactions.

The induction timer was modified with a Spellman High Voltage power source and a solid copper electrode fitted-cell. The high voltage electric field source was ordered from Spellman High Voltage Electronics Corporation and modified with wiring by the Department of Chemistry instrument shop. The couple-charged displacement (CCD) camera was purchased from Photron.

All of these components will be discussed in detail in the following sections.

3.2.1. Induction timer

The induction timer setup is based off the TFDA previously developed in the lab. Figure 22 shows an overview schematic of the modified induction timer, with various parts that were either home built, 3-D printed, or ordered from various electrical companies.

The experimental setup consists of a computer, DA/AD (digital-to-analog) amplifier, speaker, capillary tube, syringe, couple-charged displacement (CCD) camera, high voltage power source, and an electrode-fitted cell. The glass cell is fitted with the appropriate (vertical or horizontal) copper electrodes, a 3-D printed base and droplet holder, and is positioned on the induction timer base in the viewing field of the CCD camera and 40 X lens. The bottom droplet holder is aligned with a glass capillary tube which is attached to the speaker. A 12-bit DAS-16F (Omega) DA/AD board generates a desired pulse using a custom-designed computer software through sending a voltage through the speaker, resulting in an amplitude which moves the top droplet a specific distance. The CCD camera captures this motion in a high definition video of 30 frames per second, to be later analyzed using the Photron FASTCAM Viewer (PFV) software.

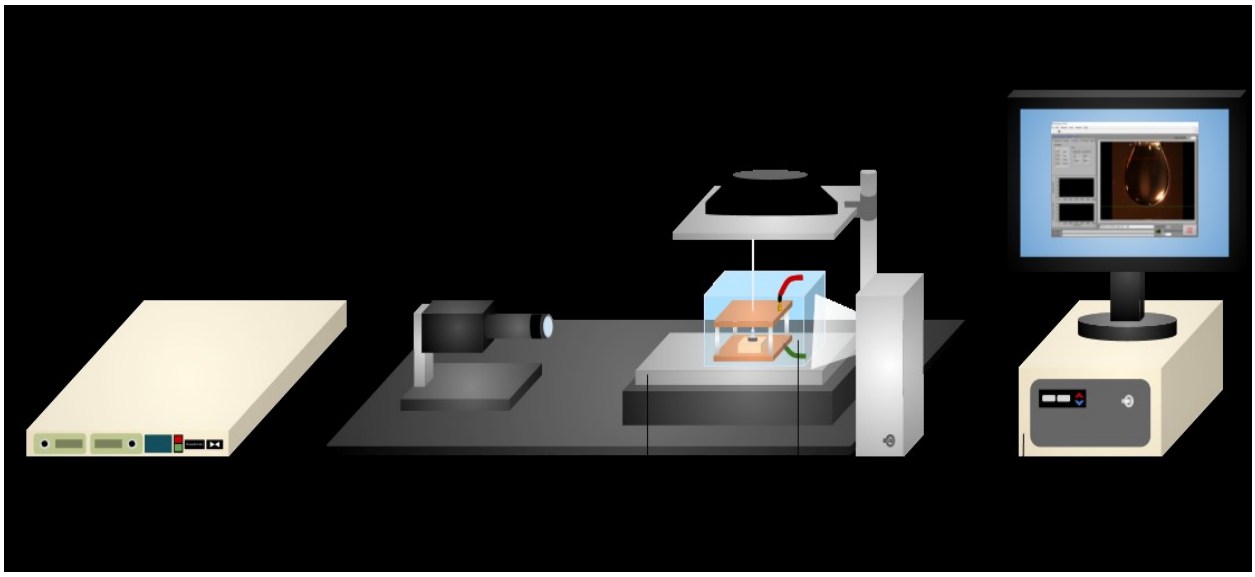

Figure 22. Schematic of modified induction timer overview.

The induction timer control system essentially powers the entire experimentation process, working alongside the high voltage power source. It acts as the on/off switch that connects to the speaker, sending a specified voltage to the speaker, which then moves the capillary tube. It also controls the temperature of the induction timer base, which can reach around 80°C (although this feature is not used in the experimentations, it can be implemented as another testing variable in future work).

3.2.2. Cell setup

The induction timer is compatible with any cell that fits in between the stand and the capillary, its original cell being made from a combination of a metal container with a glass window in order to view the experiment with a camera. For this specific experiment, the entire cell was made from glass. A glass material is ideal as it will not interfere with the electric field generated within the cell and will provide the maximum viewing area to be picked up by the camera, also allowing more light exposure within the cell. Intense light exposure is crucial as results include

the study of droplet-droplet interactions in an asphaltene-based model crude oil, which is a dark solution that makes it difficult for viewing experiments within the cell.

In order to end an electric field through the model emulsion, electrodes were required to be fitted for the cell. The electrode design needed to consist of a durable and conductive material and be compatible with the glass cell and speaker that are used with the induction timer.

3.2.3. High voltage electric field modification

A high efficiency Spellman SL Series Compact High Voltage (HV) Power Supply was used to provide an electric field for the induction timer. This model's overall output voltage ranges from 0 – 12kV. The HV Power Supply can be considered to be an AC to DC power converter; AC is converted to DC, which is further converted to high frequency AC to high voltage DC [59]. The ground cable is connected to one electrode while the positive (current) cable was connected to the opposite electrode. The HV Power Supply is grounded to the lab using the Floating Ground attachment. The overall power supply setup is pictured in Figure 23.

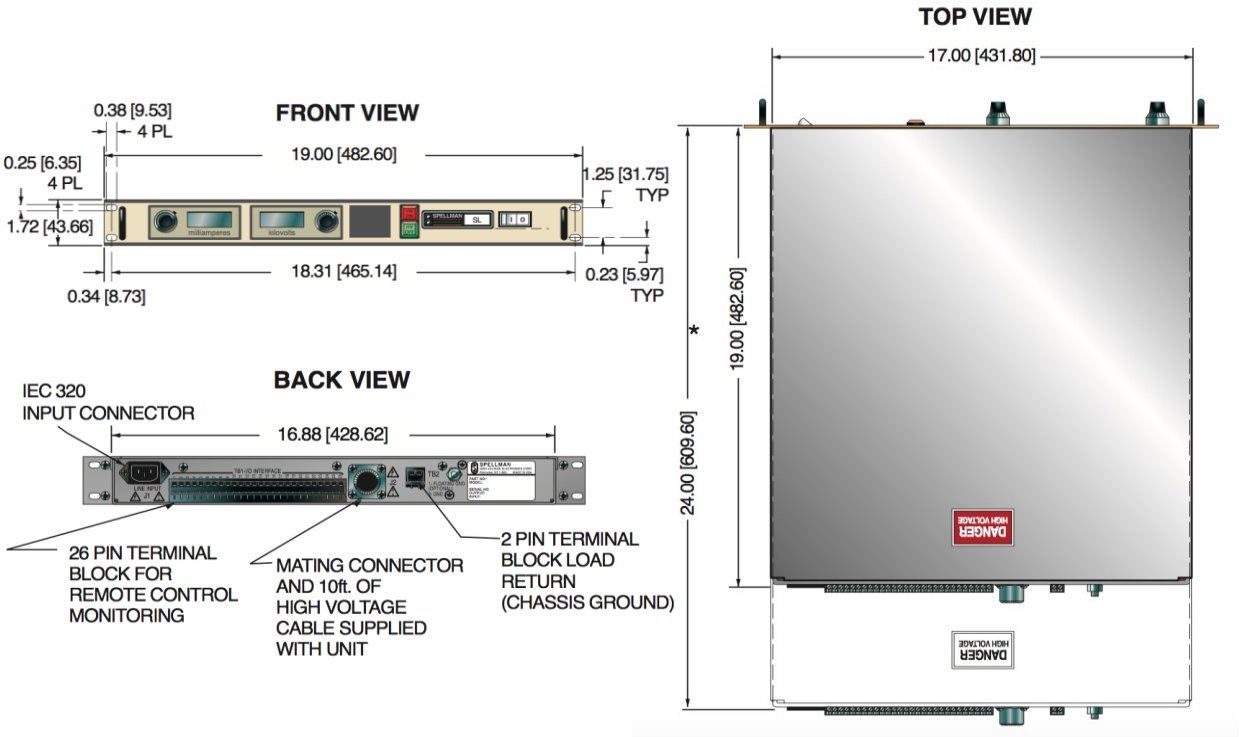

Figure 23. Schematic of Spellman SL Series Power Supply setup. [59]

The Spellman power supply allows for a modification which allows users to implement a ramp remote computer software program alongside the induction timer control program, providing precise control of ramp speed and electric field strength of the Spellman power source. This was done by using a data acquisitioner from National Instruments, and connecting it to the power source, a schematic is pictured in Figure 24.

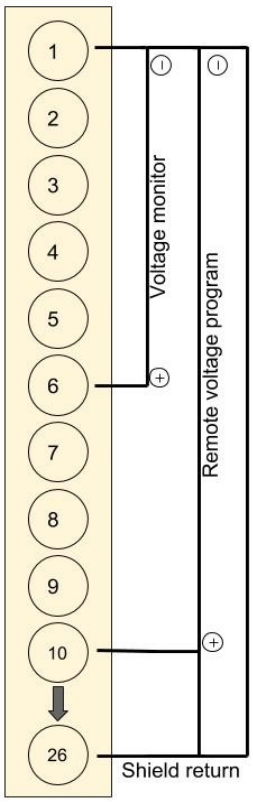

Figure 24. Schematic of ramp modification connectivity.

Data acquisition (DAQ) measures the electrical or physical phenomenon such as voltage, current, temperature, pressure, or sound with a computer, in this case, the acquisition is utilized for voltage and current [60]. The DAQ system consists of sensors which are within the HV source (connectivity pictured in Figure 24), DAQ measurement hardware, and a software programmed on the computer. Using the DAQ, a software was created that could translate the voltage to be controlled by the computer. This resulted in a "ramp voltage" software that can control the speed at which the electric field is applied to the electrode system, as well as applying the field in intervals. The remote program is pictured in Figure 25.

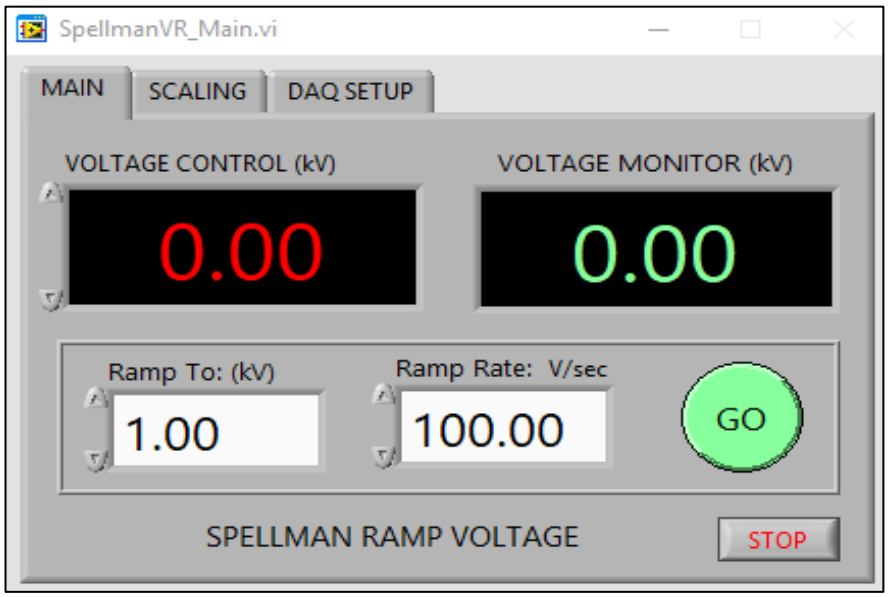

Figure 25. Image of electric field ramp voltage software.

3.2.4. Computer software

LabView is the main program used for controlling the induction timer movement, manipulating variables and placement, as well as capturing video footage of the droplet-droplet interactions. The camera viewing window is implemented into the LabView program, allowing the user to watch the experiment in real time. The program includes multiple controls for the induction timer, these include: top/bottom droplet location guides (in the camera viewer window), time to approach, time to retract, half width (known as contact time), amplitude (known as capillary distance travelled). LabView also includes a video recording function, and a measurement function which starts the experimentation process (i.e., lowering the capillary); there is also an option to start the video recording and the capillary movement simultaneously.

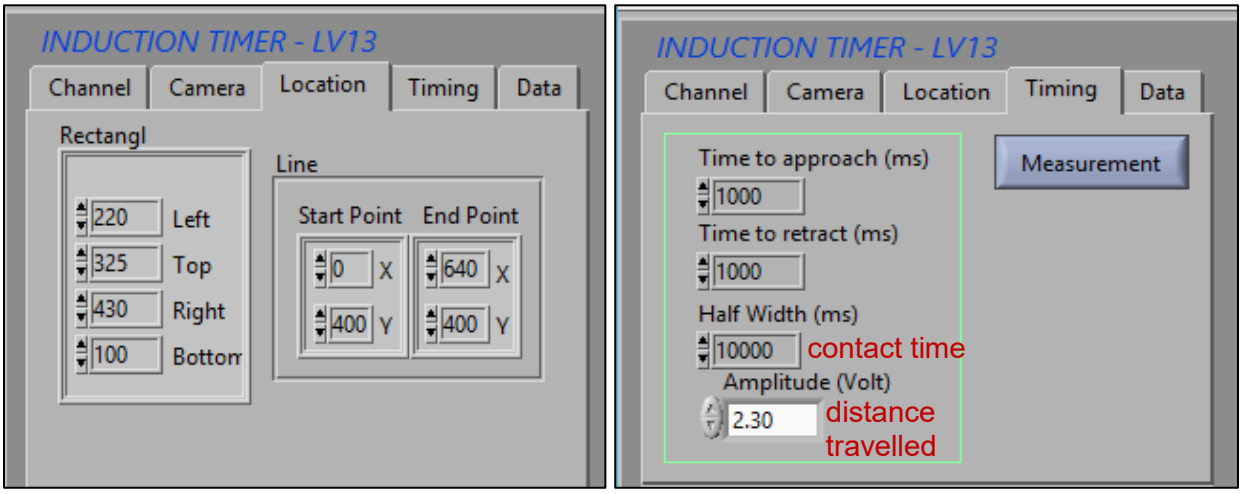

Figure 26. Images of LabView software, (a) location and (b) timing tabs with functions.

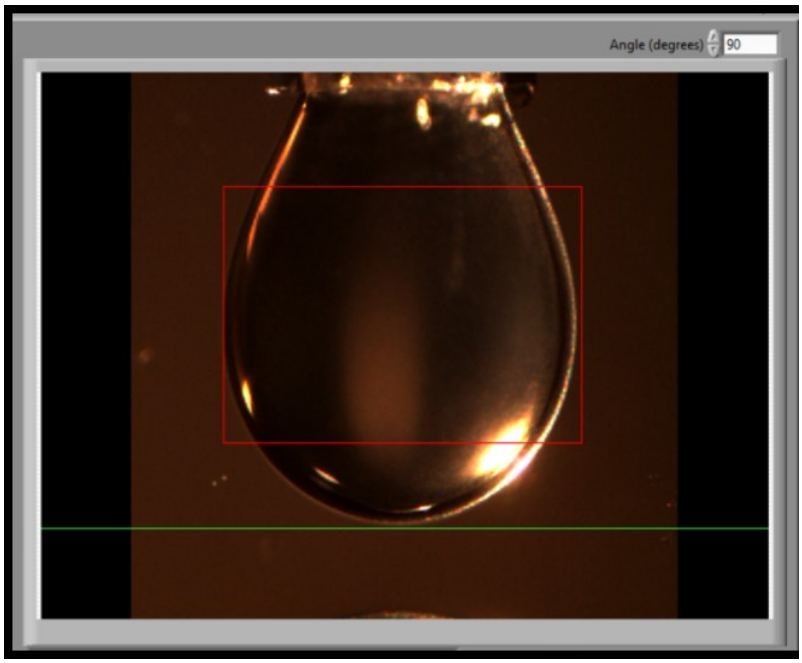

Figure 27. Image of camera viewfinder in LabView software with rectangle and line location markers.

The values in Figure 26 (a) are shown in pixels on an x/y coordinate in order to control the sizes and locations of the droplets. To convert the numerical values of pixels to units of distance, the camera viewer was calibrated using a ruler. The calibration process includes placing the ruler on a stand on the base of the induction timer, then finding and using the camera lens to focus on a section of the ruler where the lines are in view. Once in the viewfinder, a rectangle was fit over a

1 mm marking on the ruler, and the difference between the top and bottom pixels represented the pixels/mm unit conversion, which is 180 pixels/mm or 0.0056 mm/pixel.

3.3. Electrodes

The electrodes designed for experimentation are shown in Figure 28, along with their various electric source connections. These electrodes were created at the Chemical and Materials Engineering machine shop at the University of Alberta, with specific functions and characteristics in consideration.

The electrodes are made out of solid copper, with 2 cm spacing between the designated positive and ground electrodes. The horizontally designed copper electrodes are designed to deliver a vertical electric field direction, while the vertical "hanging" design copper electrodes create a horizontal electric field. These electrode sets were designed to fit in the specific glass cells used with the induction timer apparatus, as well as to be used interchangeably to test the effects of vertical vs. horizontally applied electric fields on top-bottom facing water droplets.

Teflon material was utilized for multiple parts in the electrode-cell system as metal objects that are not a part of the copper material themselves interfere with the electric field, making it non-uniform. This is not a crucial problem in the horizontal field electrodes (b), however the vertical field electrodes are more likely to produce non-uniform fields due to the necessity of corner pillars and their screws to hold them in place, as well as a top screw to anchor the upper wire that connects to the high voltage source as either a positive electricity receiving wire or a ground electricity removing wire. The copper electrodes themselves tend to tarnish or corrode over time and usage, especially since they are withstanding high electric field strengths up to 3000 volts.

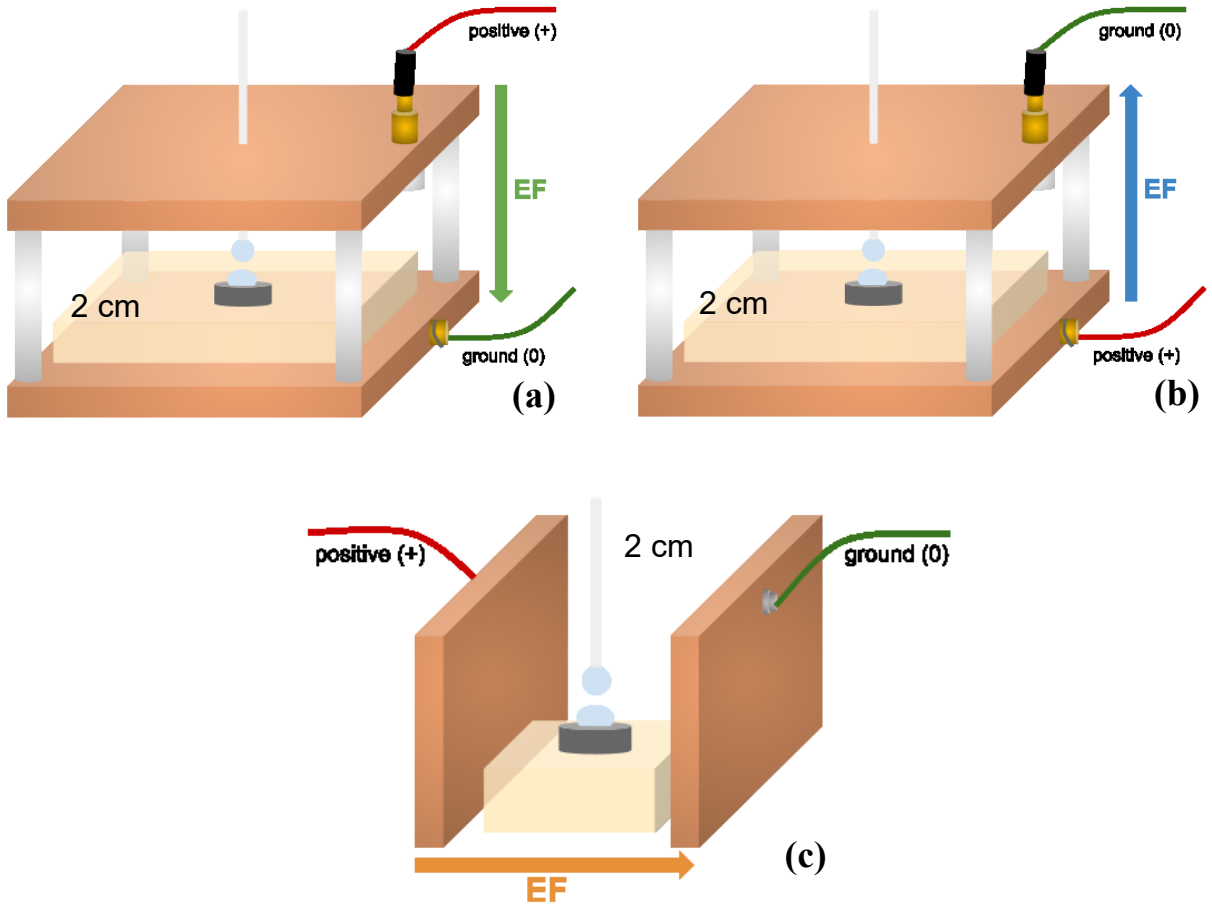

Figure 28. Schematic of (a) PG electrodes, (b) PAG electrodes, and (c) C electrodes.

3.4. Droplet positions

For experimentation, it is essential to establish different droplet position setups in order to emulate various interactions in real emulsions. There are important factors to consider when determining the droplet positions, these include the stability of the droplet film, strength of the interfacial layer, and the physical/chemical/electrical variables being studied. For the experimental results, three various positions are established. To elaborate, the stability of the droplets tells us if we can press the droplets together for a long enough period of time without resulting in immediate coalescence when the electric field is off. In order to study high voltage electric fields, the droplets must be stable enough to remain separate entities until the field is turned on for a certain period of

time, allowing us to observe and study the true effects of the electric field strength. To elaborate, a complication occurred when attempting to study the complex model oil system, where the oil phase consists of extracted asphaltenes and heptol. The film formed on the droplets was not strong enough to remain stable at droplet-droplet contact under the electric field. Even after aging the droplets in the asphaltene-based solution for over one hour, the droplets would still quickly coalesce at electric field strengths of around 100 V. Since this would result in almost instantaneous coalescence, it was difficult to extract actual times and information from the experimental videos; therefore, we would not be able to study the effects of different variables on the coalescence behavior. In order to combat this issue, we were able to study the droplets' interactions at a non-contacting setup using the asphaltene-based oil, while contacting setups were used with a clear surfactant-based model oil.

These setups were not all decided before experimentation, for instance, after discovering that electric field application time before droplet contact did not have an effect on coalescence time, the process for studying electric field application speed had to be modified so that droplets were already in contact prior to applying the electric field. As a result of these circumstances, three different setups were generated and used in different variable experiments.

Setup #1: E1 Position

E1 position is called as such since the electric field is applied first, then the droplets are later brought into contact. E1 position was the first position to be used for the majority of experiments in the research matrix, E2 is a modified version that was later generated in order to test another specific variable. This E1 position allows us to study the effects of most variables within the simple model oil experiments. Electrical variables include: electric field strength, electric field application time, electric field charge and application direction. The effect of surfactant concentration is the

chemical variable that is studied, and the physical variables studied under E1 placement are the effects of droplet overlap and droplet size.

The placement setup is described as follows:

1. Open LabView software. Align two vertical non-contacting water droplets to desired size and separation distance using camera guides. Using ramp remote control program at a controlled speed, turn electric field on, allow exposure of droplets to electric field for a set amount of time.
2. Turn induction timer on, set desired approaching and retracting speed, and contact time (half time). Start measurement and video recording simultaneously: upper droplet moves down to contact lower droplet.
3. Droplets coalesce, extract total coalescence time from video recording (frame-by-frame) using PFV Viewer program.

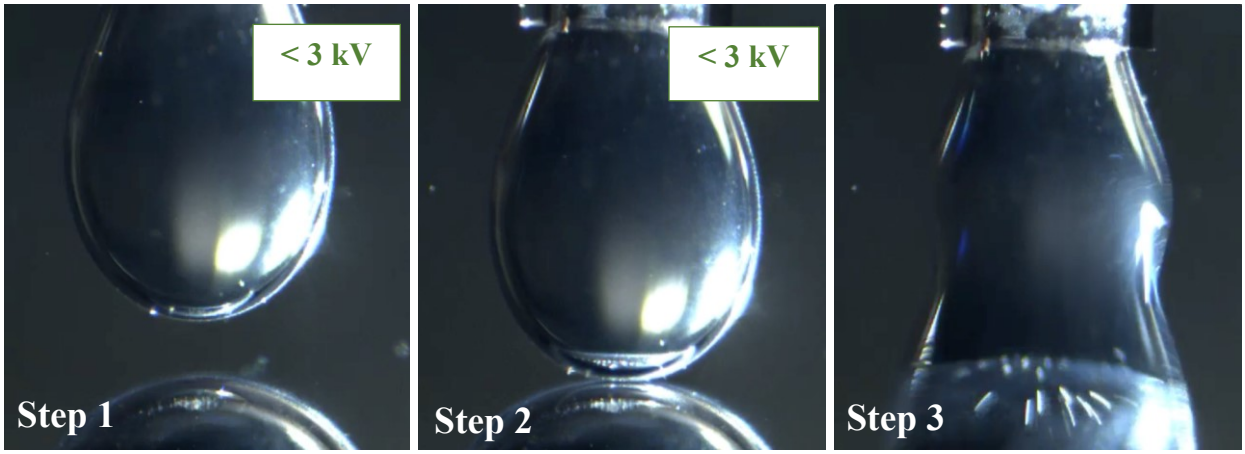

Figure 29. Images of droplets undergoing coalescence in E1 position.

Setup #2: E2 Position

E2 position is where the droplets are initially in contact, then an electric field is applied afterwards; this is the alternate version of E1. E2 was used specifically for testing the effect of

electric field application ramp speed on coalescence time, an electrical variable. This is because, in E1 position, droplets will have been separate when fully exposed to the final electric field strength before contacting one another; hence, no variable difference will be detected when measuring coalescence time after droplets are contacting. For example, assume the droplets are in a non-contacting position (as described in step 1 of the E1 setup), and are ready for exposure by the electric field, testing the effect of the ramp speed. The HV source is powered on and the ramp speed is set to 100 V/s, with the maximum field strength set as 2 kV. The HV source will require 20 seconds to reach maximum strength, and the droplets will remain in position for an extra 15 seconds to ensure full exposure before the top droplet is brought into contact with the bottom. By this time, the droplets will have either coalesced even before contact, immediately at coalescence, or after a specific contact time. The same goes for another chosen ramp speed between 10 – 200 V/s, there would be no variation as the droplets would all function at their final field strength, returning results with no variation even though the ramp speed was changed.

The placement setup is described as follows:

1. Open LabView software. Align two vertical non-contacting water droplets to desired size and separation distance using camera guides. Turn induction timer on, set desired approaching and retracting speed, and contact time (half time).
2. Start measurement and video recording simultaneously: upper droplet moves down to contact lower droplet.
3. Using ramp remote control program at variable speeds, turn electric field on right as top droplet contacts the bottom droplet.
4. Droplets coalesce, extract total coalescence time from video recording (frame-by-frame) using PFV Viewer program.

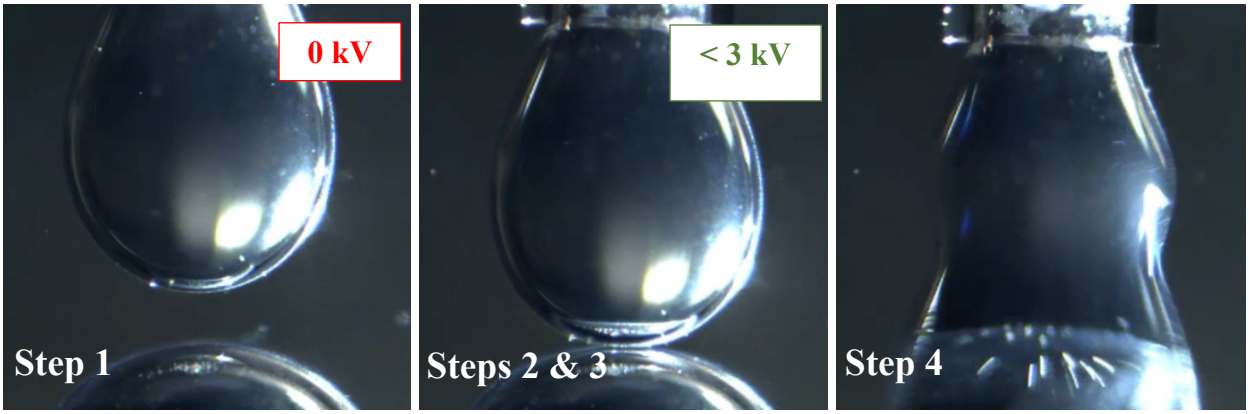

Figure 30. Images of droplets undergoing coalescence in E2 position.

Setup #3: NC Position

NC position stands for "non-contacting", where droplets remain out of contact for the entire duration of the experimental run, the electric field is turned on and allows the droplets to interact freely (while remaining in their original positions). As previously mentioned, the NC position was created in order to study asphaltene-based complex model oil, consisting of heptane and toluene (heptol) solvent, and ~0.100-0.200 g/L of extracted asphaltenes. The variables studied in NC position include the effect of electric field ramp speed (electrical variable), effect of chemical demulsifiers (chemical variable), and the effect of separation distance (physical variable), in the complex model oil.

The placement setup is described as follows:

1. Open LabView software, generate bottom droplet in teflon base and form top droplet in glass capillary, following size guides in the camera viewfinder.
2. Set separation distance and align droplets. Age droplets for ~30 minutes, turn on HV power source and set ramp speed and maximum voltage. Start electric field and video recording simultaneously.

3. Record voltage value at droplet coalescence, extract electrocoalescence time.

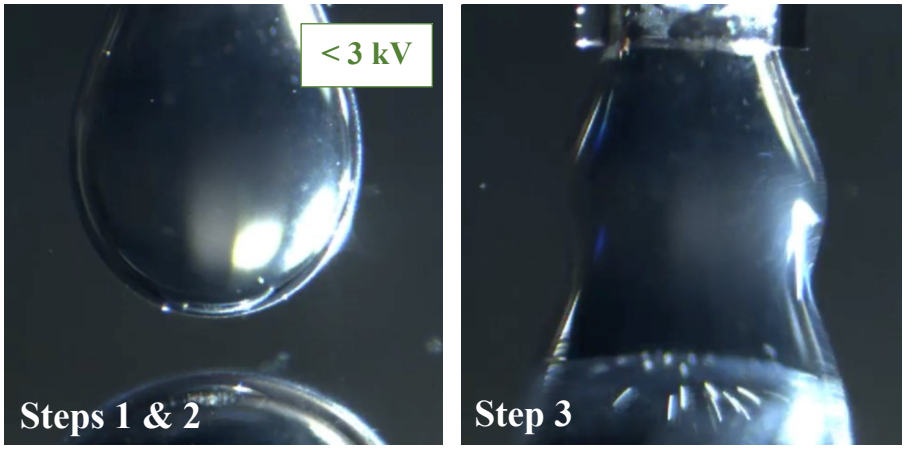

Figure 31. Images of droplets undergoing coalescence in NC position.

Chapter 4 Results and Discussion

4.1. Research flowchart

This research flowchart is used to organize and summarize the variables studied in the results.

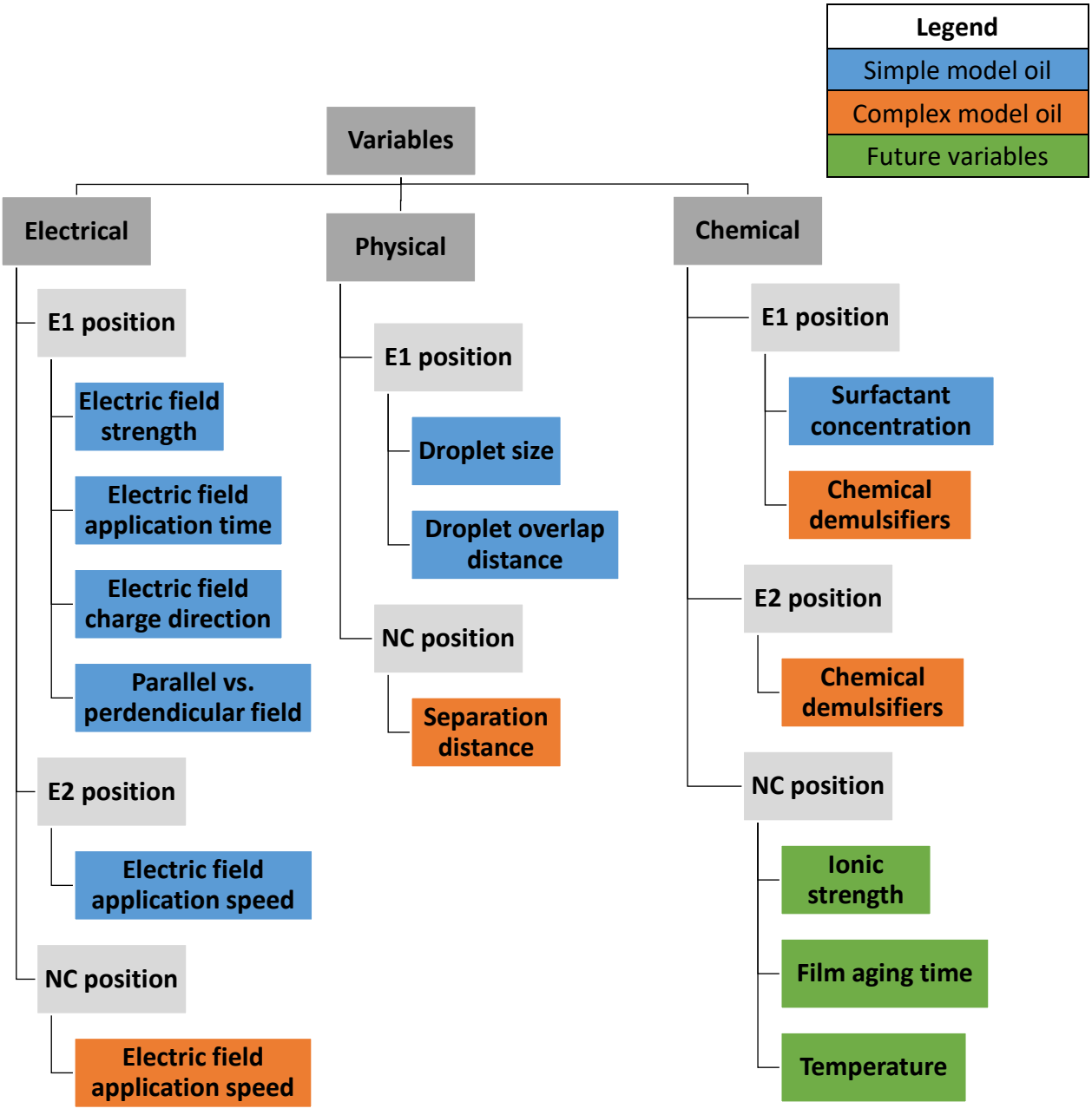

Figure 32. Research flowchart of electrical, physical, and chemical variables in E1, E2, and NC droplet positions.

4.2. Electrocoalescence properties of water droplets in simple model oil emulsion

The subchapters below discuss the results of different variables for studying electrocoalescence of water droplets in the simple model emulsion. As mentioned in Chapter 3, the water phase is made up of Milli-Q water and the oil phase is a combination of Span 80 surfactant in paraffinic ICP oil.

4.2.1. Electric field strength and shape profile

The first variable to be studied was basic application of the electric field strength. It was important to establish controlled variables, as well as to view the effects that an electric field has on a singular droplet, before examining the electrocoalescence interactions of two fixed droplets (in close proximity). As mentioned previously, too high of an electric field strength will cause droplets to burst and split into multiple, smaller bubbles. This is an undesired result that will further stabilize water-in-oil emulsions. In order to avoid this consequence, a range of electric field strengths were reviewed to visualize how droplets would react, from a minimum to a maximum range of voltages. To do this, a single droplet was formed using the capillary tube, and was placed in the center of the field in between the positive and ground copper electrodes, (both the parallel and perpendicular field electrodes).

The strengths tested ranged from 50 V to around 3.5 kV using the high voltage source and the camera to view the droplet responses. Effects that occurred included droplet stretching (both horizontally and vertically), droplet compression, swaying/stretching, vibration, and droplet splitting. At lower voltages, such as between 50 V to 250 V, there would not be visible changes to the droplet appearance or behavior. Most of these effects occurred between 500 V to 2.5 kV, with more dramatic actions nearing the higher end of this range, and splitting occurring around the maximum range of ~ 3 kV (or 1.5 kV/cm). At 3 kV, the droplet would respond the most

dramatically; either completely swaying to the positive electrode, splitting into multiple miniscule droplets, and/or detaching from the capillary itself as demonstrated in Figure 33.

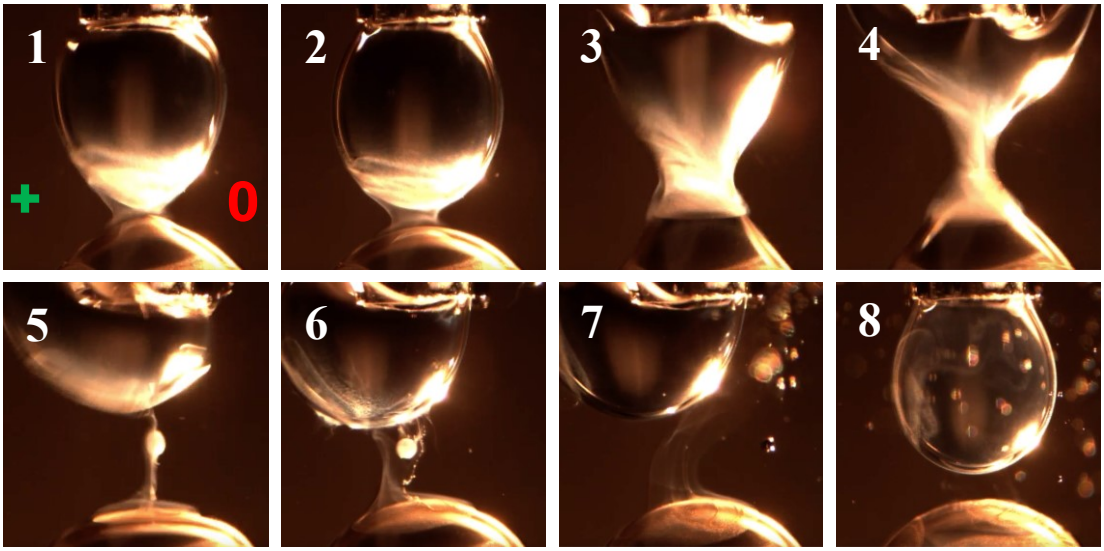

Figure 33. Water droplets in simple model oil emulsion undergoing strong swaying movement and splitting in C electrodes with ~ 3.5 kV (or 1.75 kV/cm) field strength.

Frames 1 to 4 demonstrate two droplets undergoing coalescence, however as the field remains at 3.5 kV, which is above the critical field strength of 3 kV for this system, the droplets stretch towards the positive electrode on the left side before (or while) bursting. The small resulting droplets are then visualized in frames 7 and 8.

Two droplets were then observed under the same conditions and displayed the same behaviors individually. However, when viewing responses in relation to one another, droplets would either be attracted to each other and coalesce at higher voltages, or they would repeatedly touch and display repulsive forces. Below is a figure demonstrating the various behaviors as described before. Using this knowledge, the electric field range was set around 250 V to 2 kV, as this range is where the experiments could be controlled in an effective manner, where variable, dependable, and reproducible results would be returned.

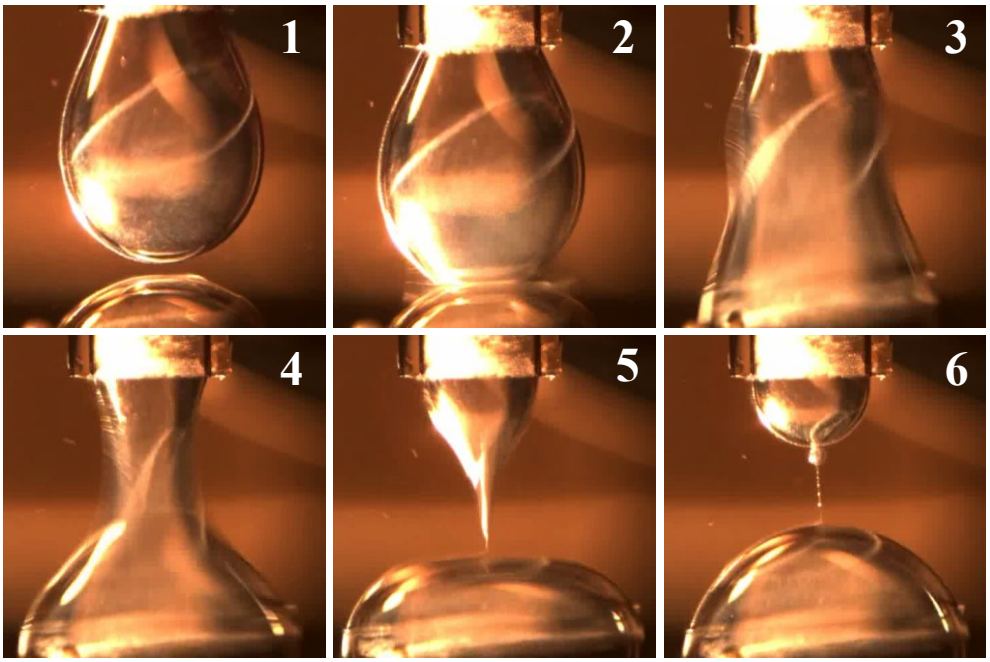

Figure 34. Images of droplet behavior under field strength of 0.25 kV/cm.

Frames are described as: 1) upper droplet manually approaches bottom droplet to contact, 2) droplets coalesce (*CT* = coalescence time), 3) *CT* + 33 ms, 4) *CT* + 66 ms), 5) *CT* + 99 ms, 6) secondary droplets after complete coalescence.

Figure 34 demonstrates the electrocoalescence process of two stationary water droplets in the simple model oil emulsion in an electric field of 0.25 kV/cm. The process initially starts with the upper droplet manually approaching the bottom droplet using the LabView software until both droplet surfaces come into contact with 0 mm overlap. The droplets coalesce and continue to undergo various shape changes, from the initial film drainage, following by a thick neck, which thins out until it forms a cone shape, then finally detaching from the glass capillary and merging with the lower droplet. As shown in frame 6, a small droplet is left from the coalescence process, which then either coalesces into the nearest droplet or is pulled to the positive electrode, if the electric field is still turned on. The surfactant layer is visible in the screenshots, however there is not much displacement of the layer, showing that the main contributing forces come from the

electric field itself while the interfacial layer maintains its' viscoelasticity, resulting in a higher electrocoalescence time at 0.25 kV/cm as compared to the following examples.

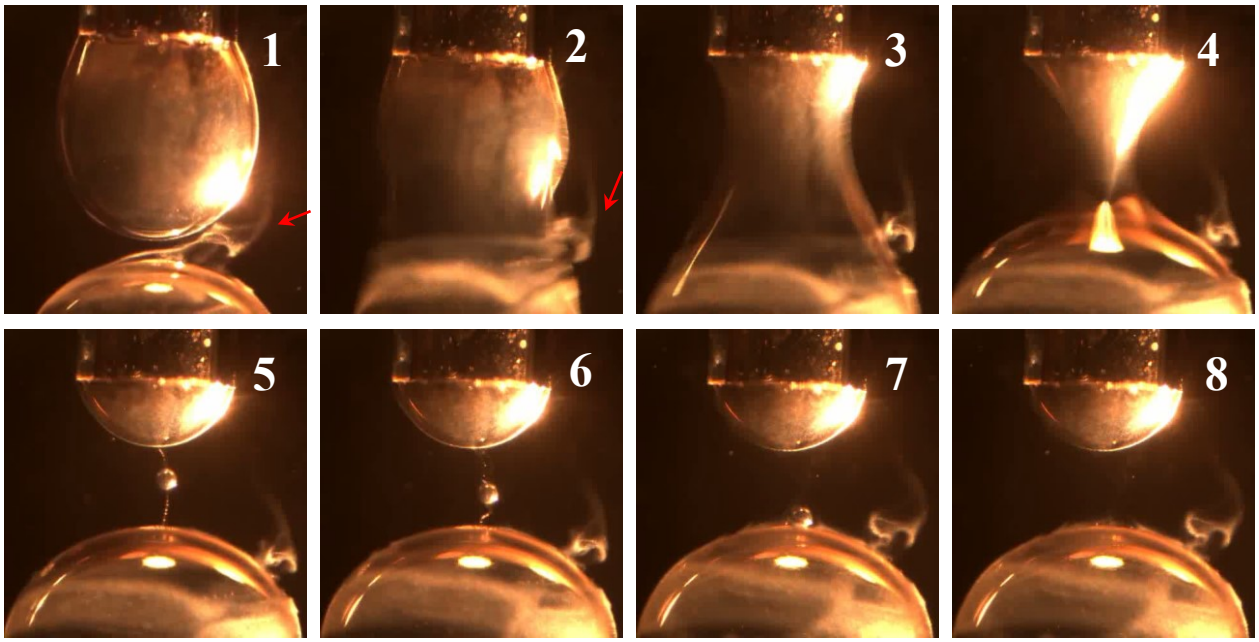

Figure 35. Images of droplet behavior under field strength of 0.50 kV/cm.

In Figure 35, frames are described as 1) upper droplet manually approaches bottom droplet to contact, 2) droplets coalesce (CT = coalescence time), 3) CT + 33 ms, 4) CT + 66 ms), 5) CT + 99 ms and secondary droplet forms after complete coalescence, 6-8) secondary droplet coalescing. We can see that the surfactant layer is being displaced in frames 1 & 2 (red arrow). The droplets then undergo a similar shape transformation as described in Figure 34, with a resulting secondary droplet and some stringing droplets aligned in the direction of coalescence. The displacement of the Span 80 surfactant results in a reduced viscoelasticity of the oil phase and the interfacial layer between the two droplets. The main contributors here include the Coulomb force (F_C) resulting from the charge of the droplets and the electric field is a major contributor, electric forces acting on the droplet, and displacing the interfacial layer all work to increase drop-drop interaction and

reduce electrocoalescence time. Rigidity of the droplet remains controlled here as the critical electric field strength has not been reached, hence, there is no major deformation or reduction in interfacial tension between each droplet and the organic phase, electrocoalescence is achieved in a shorter time.

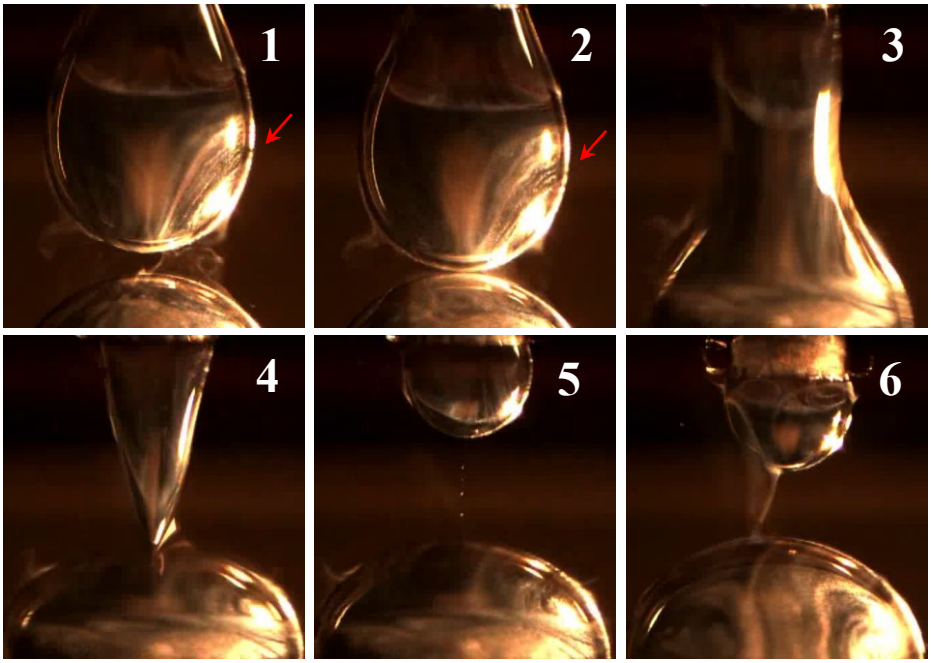

Figure 36. Images of droplet behavior under field strength of 1.00 kV/cm.

In Figure 36, frames are described as 1) upper droplet manually approaches bottom droplet to contact, 2) droplets coalesce (*CT* = coalescence time), 3) *CT* + 33 ms, 4) *CT* + 66 ms), 5) *CT* + 99 ms and stringing droplets form after complete coalescence, 6) surfactant displacement. The surfactant displacement is displayed in frame 1 (red arrow), showing the surface lines that seem to follow the direction of the electric field lines and the viscosity in the interfacial layer. Coalescence occurs in frame 2 and film drainage shapes are visible from frame 3 to 4, similar to those of electric field strengths of 0.25 and 0.50 kV/cm.

The following data was obtained by following droplet setup #1, the E1 position, using the PG electrode system. Controlled ~ 1.3 mm diameter droplets were exposed to various electric field strengths for 15 seconds and then brought into contact with ~ 0 mm overlap until coalescence, this was repeated for multiple trial runs.

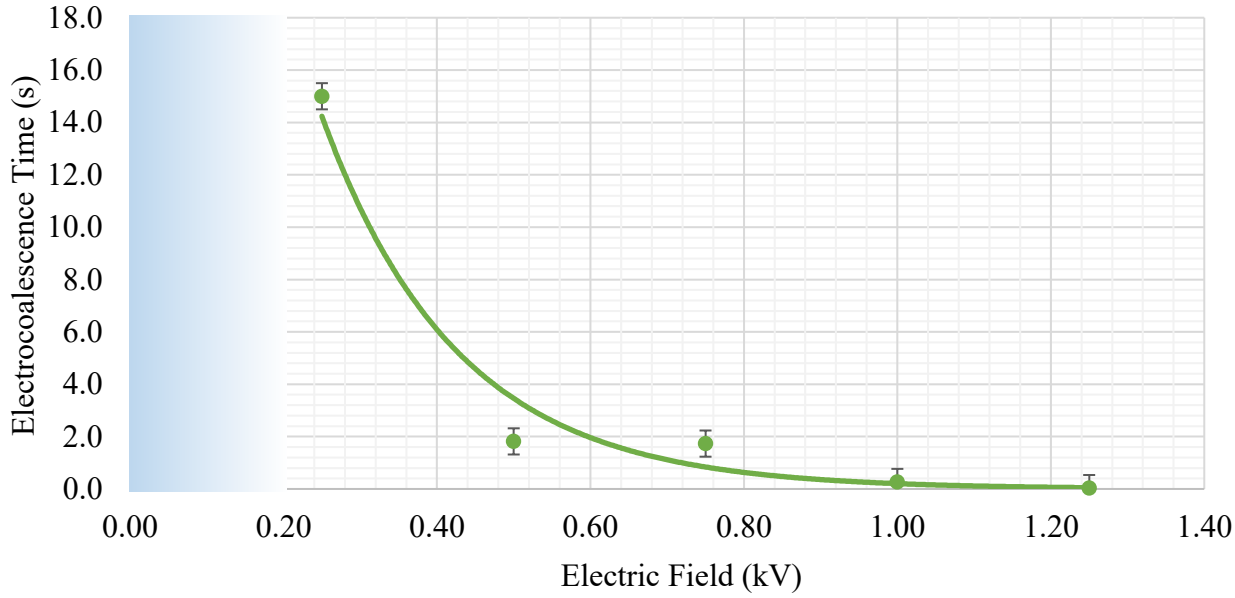

Figure 37. Graph of electrocoalescence time (s) as a function of electric field strength (kV) in PG/E1.

Overall trends demonstrate that coalescence time decreases with increasing electric field strength, up until a critical voltage. There are different voltages that are specific to each individual system, in this system specifically, electric field strength ranging from > 250 V to a maximum of around 1.5-2 kV. The light blue shaded are represents “no coalescence” as the electric field strength is not sufficient enough at these voltages in order to make a difference in the droplet-droplet coalescence time in the system. At strengths greater than 1.25 kV, coalescence time continues to occur immediately at contact between droplet surfaces after being exposed to the electric field. As seen previously, droplet stringing occurs at strengths around and greater than 3

kV, therefore, the graph does not include a trendline following ~ 2.5 kV. We can assume that for this electric field system setup, generally, coalescence time should increase beyond 2.5 kV due to the large quantity of newly formed smaller droplets. This is unable to be measured as the newly formed droplets are no longer attached to the capillary tube or positioned in the base stand; furthermore, if the electric field is turned on, droplets are rapidly moving throughout the cell in the direction towards the positive electrode, making the system increasingly difficult to control in order to measure coalescence times.

As stated by Mhatre (2018), application of an electric field induces dipolar attraction between droplets while also deforming the coalescing droplets. As the droplets approach the electric stresses at their inner faces build up and the faces assume conical shape as shown in frame 4 of Figure 36, which reduce the resistance to the film drainage.

4.2.2. Parallel vs. perpendicular direction of electric field application

The next variable studied was the direction in which the electric field acts on the droplet. This is done by comparing the effect of the cross (C) electrodes versus the parallel gravity (PG) electrodes on the electrocoalescence time of the droplets. The difference here is that the electric field can either be acting in the direction of droplet movement (PG electrodes) or perpendicular to the movement of the droplet. The electrodes referred to are illustrated earlier in Figure 28, images a) and c).

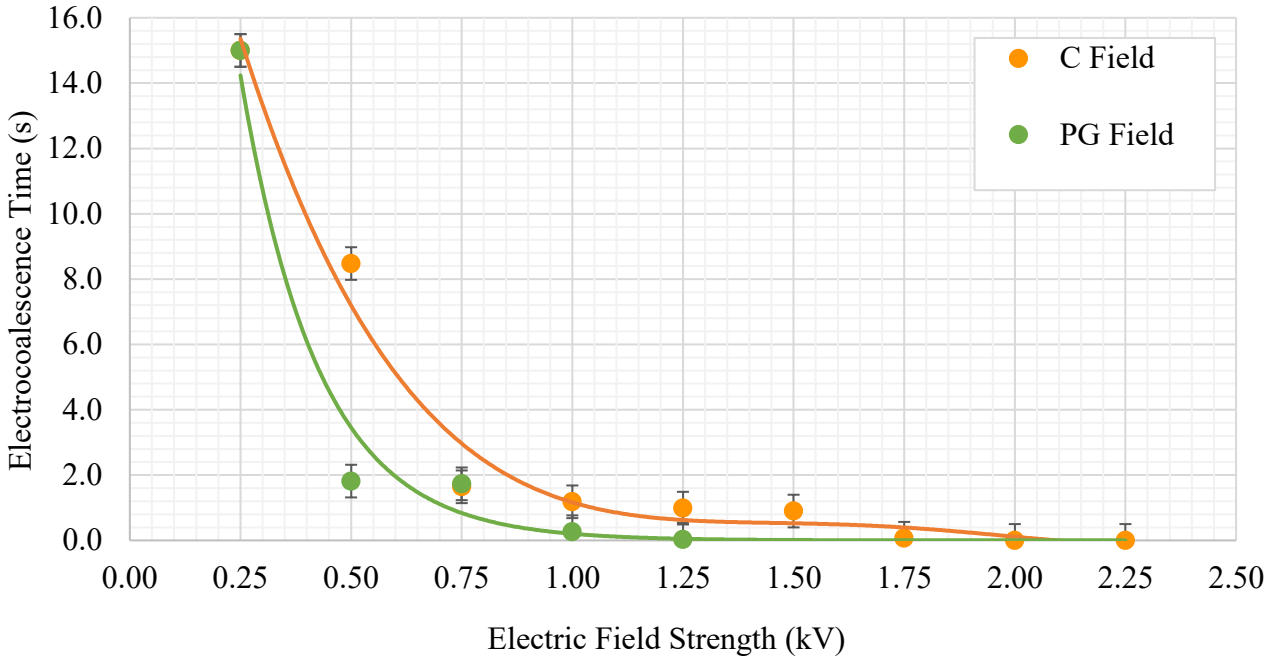

Figure 38. Graph of electrocoalescence time (s) as a function of electric field strength (kV) in PG/E1 and C/E1.

The graph shows that the trendlines of the two setups, PG/E1 and C/E1, are not distinctively different. However, the trendline for PG is slightly shifted towards the left, meaning that the electric field strength required to achieve faster electrocoalescence time is lower, which is a favorable outcome. Hence, applying the electric field in the same direction as droplet movement, if achievable, is preferential but not critical.

4.2.3. Duration of electric field application time

In E1 droplet position, we have the option to vary the application time of the electric field on the droplets before they contact. This is a useful variable to analyze in order to find out exactly which aspects of electric fields are dominating forces on droplet interactions, using the E1 position where droplets are initially exposed to the electric field prior to contact. Throughout other E1 experiments, electric field was applied to the droplets for a controlled interval of 15 seconds before

measuring coalescence times. For these experiments, the application time was varied, while all other variables were controlled. Different application times were also varied under three different electric field strengths; combining these system properties allows us to study how these variables respond in relation to each other.

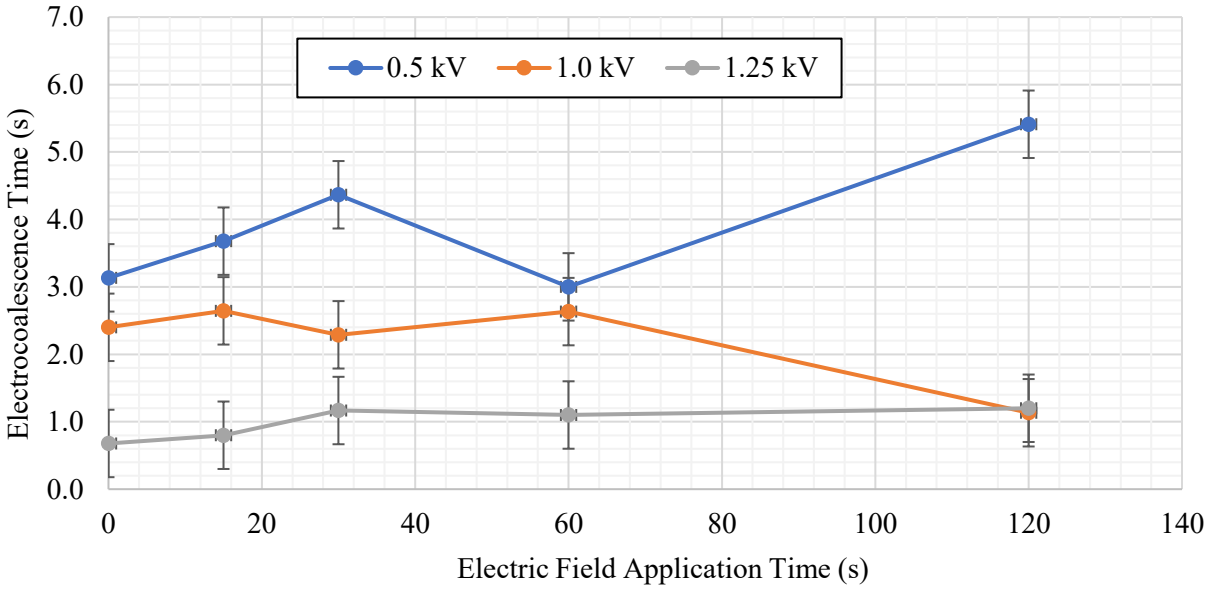

Figure 39. Graph of electrocoalescence time (s) as a function of electric field application time (s) in PG/E1.

The graph demonstrates the trendlines of two droplets in PG/E1 with varying electric field application time, using electric field strengths of 0.5 kV, 1.0 kV, and 1.25 kV. As shown in the graph, there is not much variation in the trendlines within the range of the different application times or 0 s, 15 s, 30 s, 60 s, or 120 s. Most electrocoalescence time values fall within a two second range, with no specific trends indicated. The fluctuations are mostly due to systematic errors within the experiment. This can include further aging the droplet while applying the electric field for a longer time. There appears to be little correlation between the data points in each voltage, however, the location of the various field strength trendlines on the y-axis confirm that the electric field

strength does indeed reduce electrocoalescence time. The trendline for 0.5 kV strength data shows a range between 3.0 to 5.0 seconds, this is dropped to ~ 0.7 to 1.2 seconds under a higher field strength of 1.25 kV.

4.2.4. Electric field charge direction

The next variable studied is the direction of the electric field application using the PG and the PAG electrode systems, both in E1 droplet position to ensure controlled results. This variable was tested in order to verify whether or not the direction of application, following or opposing the direction of gravity, would have an effect on the droplet interactions and hence coalescence time itself. All other variables remained constant, both droplets were placed in the middle of the electric field area of 2 cm, while positive and ground wire connectivity were switched.

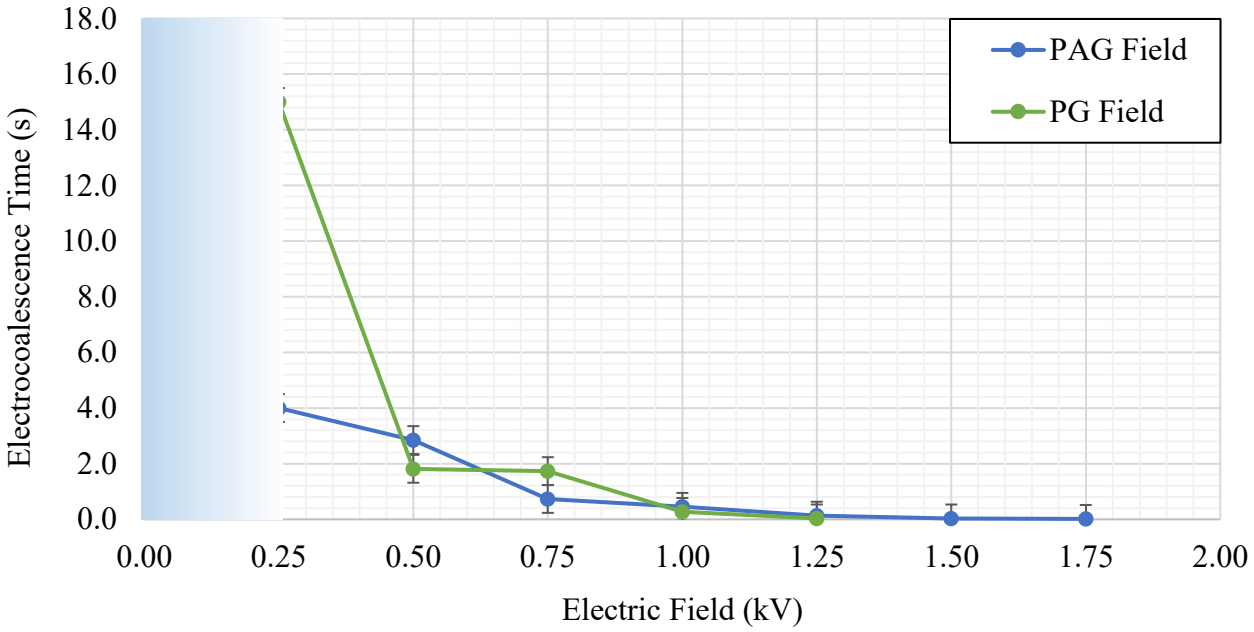

Figure 40. Graph of electrocoalescence time (s) as a function of electric field strength (kV) in PG/E1 and PAG/E1.

Overall, changing the direction of electric field application between gravity (G) and anti-gravity (AG) demonstrates no significant variation between trendlines of the system electrocoalescence times at higher electric field strengths. Gravity did not play a significant role in the force acting on the PG droplet coalescence as PAG returns similar results, hence, we may conclude that the main dominating force in this system is the electric force or stresses. If we were to quantify any minor variation due to the assistance of the pull of gravity in this system using PG electrodes, it would occur during lower electric field strengths less than 1 kV. This may be due to the upper droplet's downward movement towards the lower droplet, so the fact that the bottom electrode exhibits a positive charge may assist in the directional movement and hence vary the electrocoalescence time. Even so, higher electric field strength appears to be the main contributing variable in the efficiency of electrocoalescence time, so lower electric field strengths will not be very beneficial to a system requiring phase separation, which concludes that the direction itself is a negligible condition in higher electric field strengths.

4.2.5. Electric field application ramp speed

Manipulation of the electric field application speed was conducted by using the high voltage source ramp program. Controlling the speed at which the field is applied to a W/O emulsion system is not commonly studied, and with a few experimental runs, there was enough variation between drop-drop behaviors to confirm that it is in fact a critical variable to look into. The setup was done using the PG electrode system as it was the preferred system for most experiments. There were also various droplet position methods to choose from in order to visualize which method worked best with varying ramp speed. With E1, the droplets are exposed to the electric field for 15 s before coming into contact. This leaves room for error as the droplets may coalesce within this time frame, varying the method of droplet interaction. Hence, using an E2 method, where droplets are already

in contact (and non-coalescing) once the electric field is turned on and ramped up as the desired speed and strength.

The method of experimentation was to set up the droplets in the E2 position and set the maximum electric field strength to 3 kV (or 1.5 kV/cm), which is the E_c determined for this system. The ramp program was started at the moment of droplet contact, so that the coalescence time could be measured simultaneously. Various application ramp speeds of 20 V/s, 40 V/s, 60 V/s, 80 V/s, and 100 V/s were studied, and the times and voltage of coalescence were recorded and graphed in Figure 41. The electrocoalescence voltage is the strength of the electric field at which the droplets coalesced, this value varied as a result of the different application speeds.

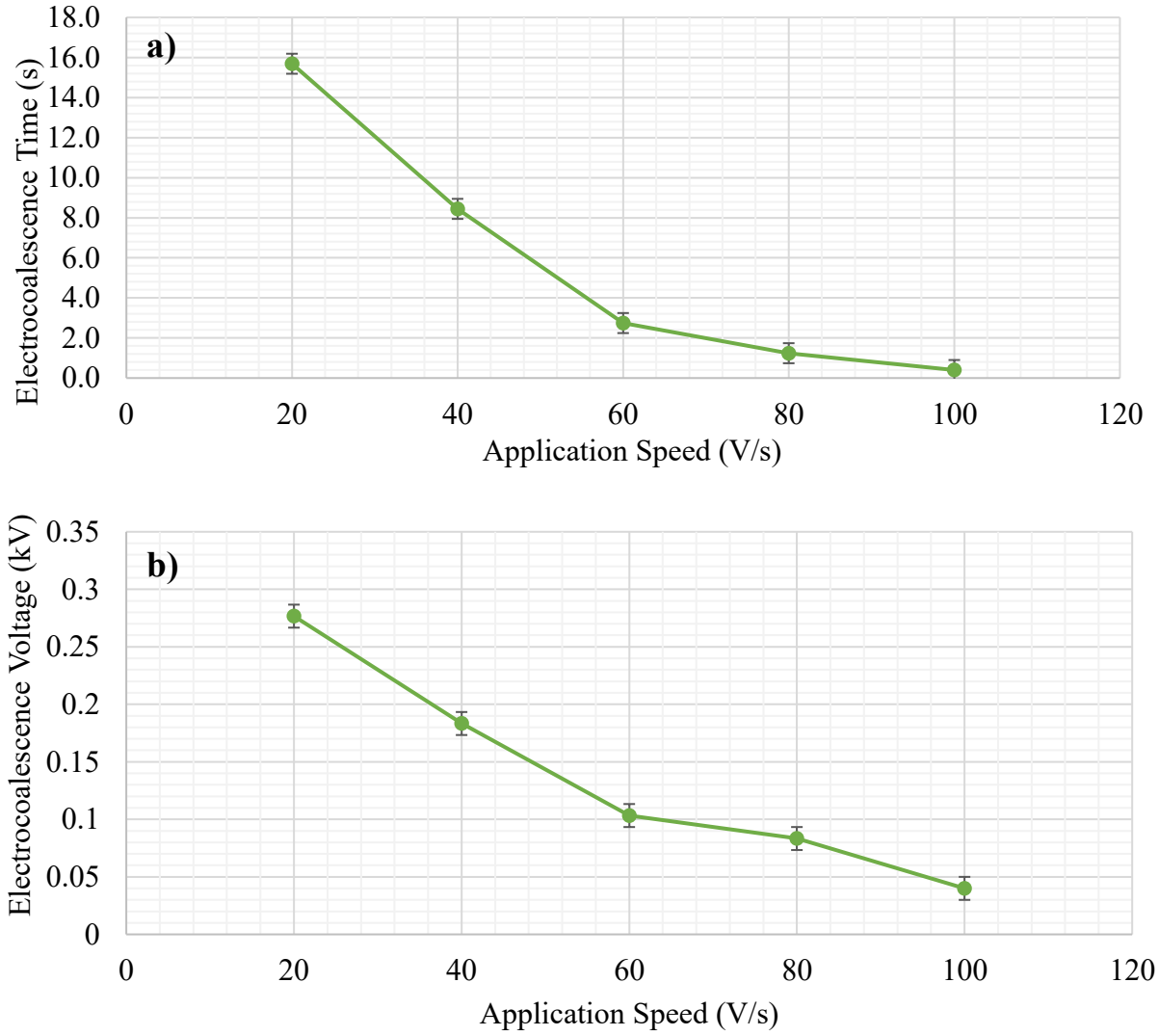

Figure 41. Graphs of (a) electrocoalescence time (s) and (b) electrocoalescence voltage (kV) as a function of electric field application ramp speed (V/s) in PG/E2.

Graph (a) indicates that the electrocoalescence time decreases with increasing speed of electric field application speed, which is a favorable outcome since it will take less time to achieve phase separation through higher speeds. Graph (b) indicates the same relationship in which an increasing electric field application speed will result in lower voltage strengths required for electrocoalescence to occur. Therefore, this outcome is favorable on both sides, lowering the voltage and the time required for droplets to coalesce in an electric field with increasing the application speed. These graphs are co-dependent, so their values correspond to one another.

For instance, at field application speed of 20 V/s, droplets coalesce at 0.276 kV after 16 seconds of contact time. Application speed is a crucial variable in the case when droplets are already in contact (E2 droplet position) once the electric field is turned on.

4.2.6. Surfactant concentration

As discussed in literature review, higher surfactant concentration between droplets is expected to result in slower coalescence time, due to the increased viscoelasticity in the interfacial layer which decreases surface interactivity between droplets. For these experiments, two distinctive concentrations of Span 80 were studied in order to visualize if this is the case along various electric field strengths that have been used in the previous sections. The resulting data is graphed below in Figure 42.

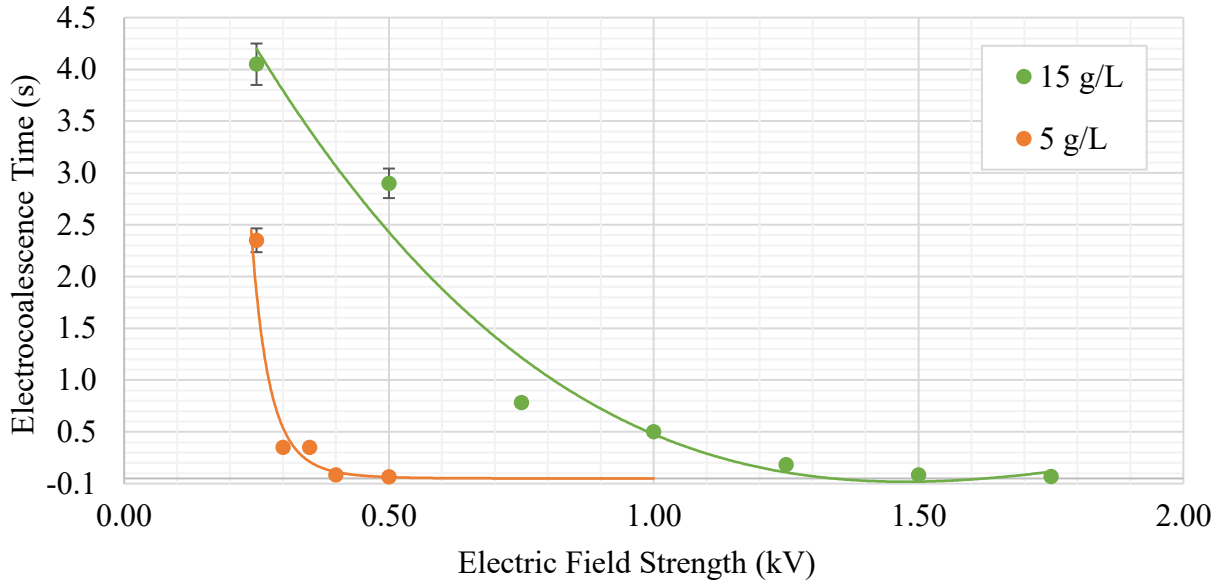

Figure 42. Graph of electrocoalescence time (s) as a function of electric field strength (kV), with varying Span 80 concentration in PG/E1.

As demonstrated with the 15 g/L trendline, there is a shift towards the right side as compared to the 5 g/L trendline, showing that a higher electric field strength is required in order to decrease

electrocoalescence time. With the 5 g/L trendline, the E_c is reached much earlier around 0.5 kV, before electrocoalescence time does not decrease and possible unwanted bursting effects occur. Compared to the 15 g/L, the E_c occurs at around triple the strength, which is shown to be around 1.5 kV. This is an interesting relationship as the smaller surfactant concentration of 5 g/L is 1/3 the concentration of the higher concentration of 15 g/L. Overall, trends in this graph agree with previous studies in which electrocoalescence time is delayed with increasing surfactant concentration.

4.2.7. Droplet size

Droplet size is an important variable that is proven to directly affect coalescence time through the Laplace equation, according to which, a larger droplet will cause a decrease in interfacial tension due to the droplet's pressure distribution. Therefore, the droplet surface is more readily deformed, attracting more dimples in the interfacial layer which traps the organic phase, thus further complicating the coalescence process.

It is important to study if these claims remain valid for W/O droplets within an electric field, as other subchapters have shown that the electric force is a major contributor that triggers coalescence. If the electric force is the main contributor, then we will expect no variation among the electrocoalescence times and behavior between the different droplet sizes.

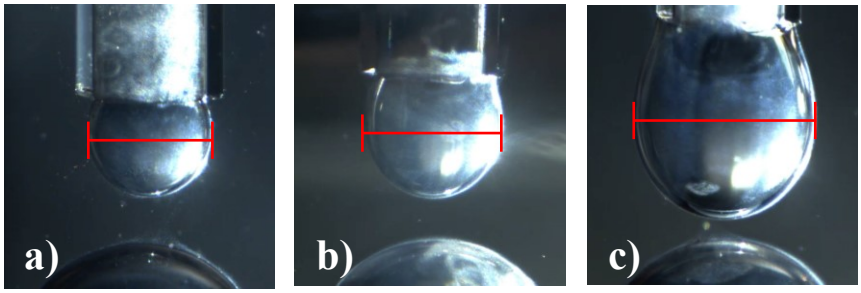

Figure 43. Images of various sized upper droplets in simple model oil with diameters of a) ~1.1 mm b) ~1.3 mm c) ~1.7 mm.

$\Delta p = 2\gamma/r$ is the Young-Laplace equation for two droplets of the same radii, while $\Delta p = \gamma\left(\frac{1}{r_1} + \frac{1}{r_2}\right)$ is used for two different radius values. In these experiments, the lower droplet radius is maintained at a constant size of ~0.85 mm, while the upper droplet sizes were varied with diameters of 1.1 mm, 1.3 mm, and 1.7 mm (or radii of 0.55 mm, 0.65 mm, and 0.85 mm, respectively). If the radius is varied between the range of values, Young-Laplace shows the following relationship with r_1 representing the lower drop and r_2 as the upper drop. Interfacial tension and pressure difference remain variable.

$\Delta p = \gamma\left(\frac{1}{r_1} + \frac{1}{r_2}\right)$ the greater the increase of radius values, the lower the interfacial tension must be in order to maintain a constant pressure difference, resulting in "softer" droplets when studying larger radii that are easier to deform and more readily trap the oil phase in the interfacial layer. Using real values from experimentation, we have:

Largest upper droplet: $\Delta p = \gamma\left(\frac{1}{0.85} + \frac{1}{0.85}\right) = 2.35\gamma$

Smallest upper droplet: $\Delta p = \gamma\left(\frac{1}{0.85} + \frac{1}{0.55}\right) = 2.99\gamma$

These relationships demonstrate that we can expect the interfacial tension to decrease with increasing radii, and that the pressure difference is lesser within larger droplets, therefore making them more unstable, easier to deform, and hence more likely to trap an interfacial film layer.

The equation $\mathrm{E_c} = 0.648\sqrt{\frac{\gamma}{2\varepsilon r_0}}$ was derived in literature to calculate E_c, the critical electric field value, at which the droplet breaks up.

Largest upper droplet: $\mathrm{E_c} = 0.648\sqrt{\frac{\gamma}{2\varepsilon\,(0.85)}} = \frac{0.50\gamma}{\varepsilon}$

Smallest upper droplet: $\mathrm{E_c} = 0.648\sqrt{\frac{\gamma}{2\varepsilon\,(0.55)}} = \frac{0.62\gamma}{\varepsilon}$

The above relations mean that the greater the droplet radii, the lower the critical electric field value is, indicating that larger droplets will be more easily deformed in an electric field as well.

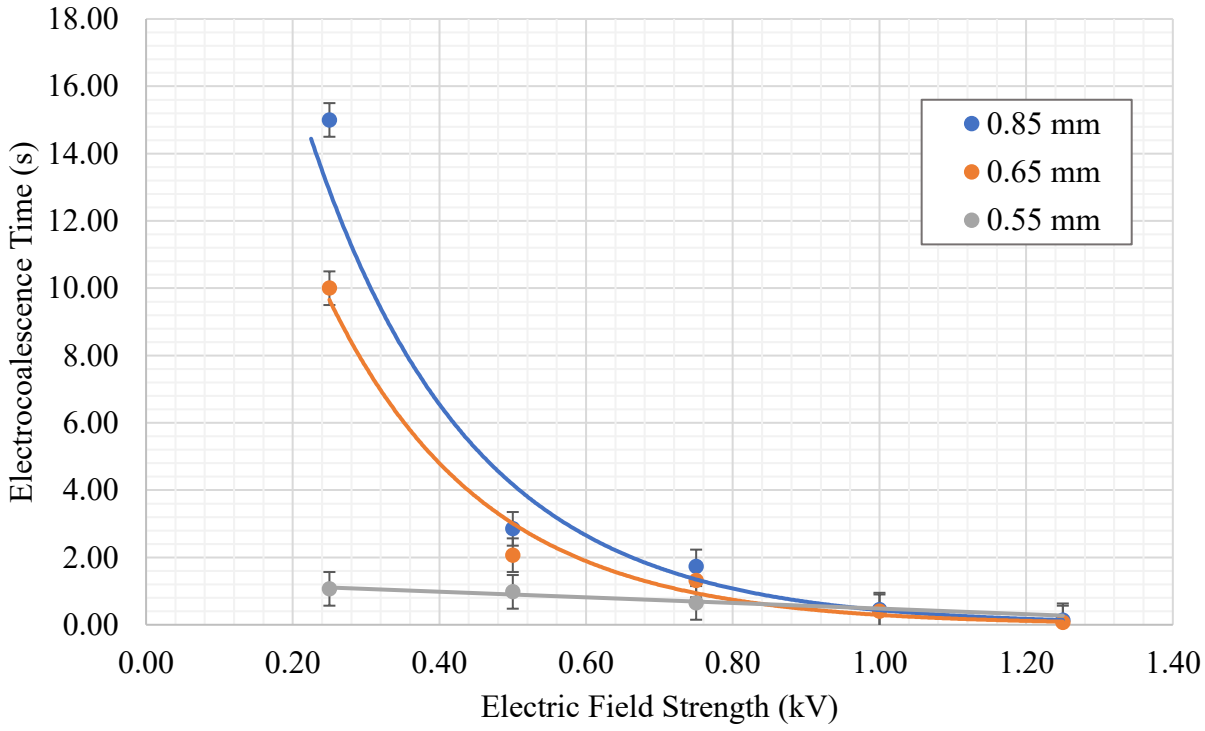

Figure 44. Graph of electrocoalescence time as a function of droplet diameter in PG/E1.

As shown in Figure 44, the largest droplet radius of 0.85 mm requires the most time in order to undergo electrocoalescence, while the smaller droplets coalesce faster, with the smallest radius

of 0.55 mm coalescing at < 2 s. In the relations shown above, this is expected as larger droplets deform more readily, lowering interfacial tension and trapping the oil phase in the thin film between the droplets, reducing drop-drop interactivity. Hence, a higher electric field strength is required in order to achieve electrocoalescence. However, this observation does not seem correct at first after evaluating above that the larger droplet radius results in a lower critical electric field. To explain this discrepancy, the above relationship refers to a single droplet in an electric field, in which the initial radius does affect the critical electric field that a droplet may withstand before bursting at greater strengths. However, this phenomena changes with two droplets, as the major contributors include the weakened interfacial tension and the trapped layer due to the dimples formed by the easily deformed larger droplets. Therefore, it is important to establish this difference as a strong electric field may be required to induce electrocoalescence between two droplets with larger radii; however, too high of a voltage may result in surpassing those droplets' E_c, which can cause premature droplet splitting if the droplets are not close enough in proximity in order to engage in electrocoalescence, which is highly unfavorable.

4.2.8. Droplet overlap

The degree of droplet overlap is a variable that can be readily studied in the experimental setup as it is easy to control the movement of the droplets, as well as the speed. One may assume that the greater the force that presses the droplets together, the more likely they are to coalesce, which should result in faster coalescence time. However, evaluating the properties and behavior of the thin film should be prioritized, as it plays a large role in the stability of the droplets. The schematic in Figure 45 shows a possible model of two overlapping droplets trapping an interfacial layer.

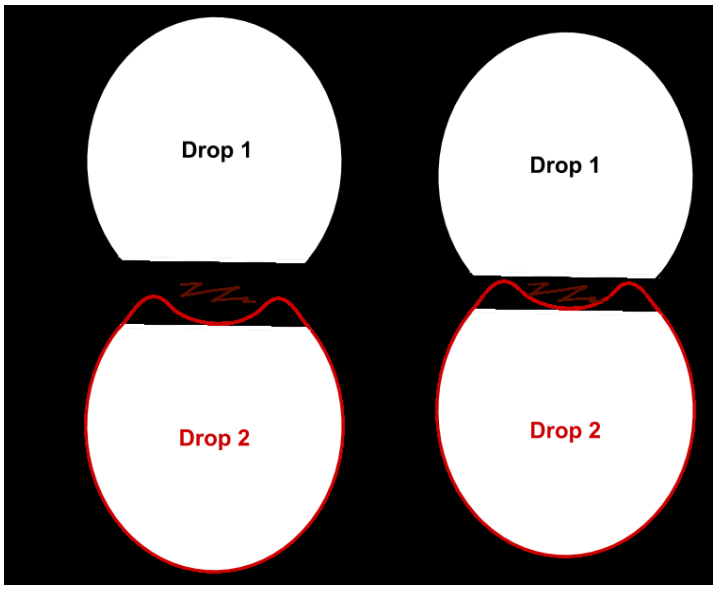

Figure 45. Schematic of two overlapping droplets trapping interfacial layer.

In the first scenario of Figure 45, the droplets are not overlapping and allow film drainage to occur as their surfaces begin to interact. In the second scenario, droplets are overlapped to a greater degree, thus trapping the film in between and reducing surface interactivity.

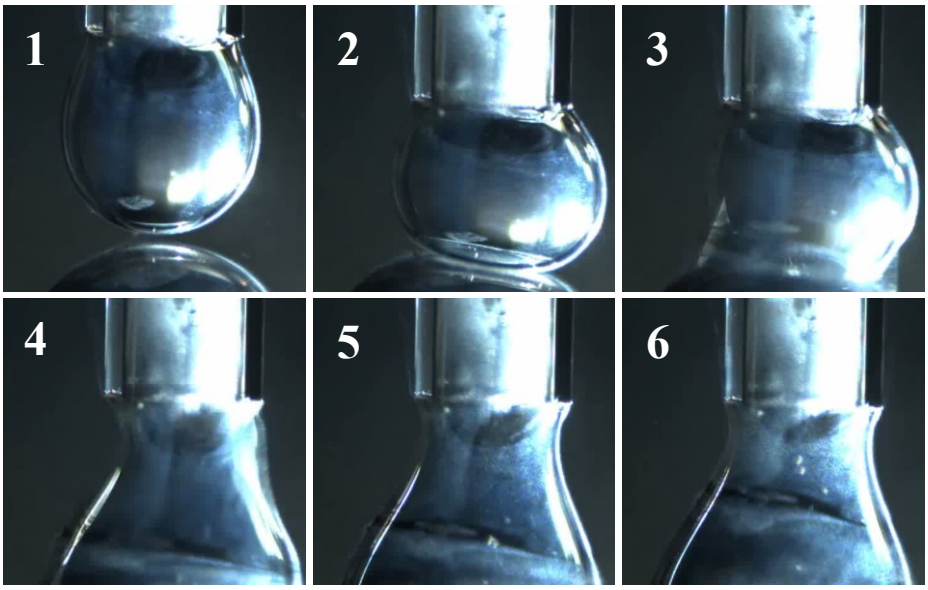

Figure 46. Images of overlapping water droplets in an electric field strength of 0.50 kV/cm at 1) position before contact, 2) maximum overlap of 0.40 mm, 3) coalescence time (CT), 4) CT + 33 ms. A trapped interfacial layer is viewed in images 5 and 6.

The above images demonstrate the process of droplets undergoing electrocoalescence after reaching maximum overlap. As viewed in frames 4 to 6, the interfacial film is shown as a line in between the coalesced droplets. This is highly unfavorable as the overlapping droplets trap the organic phase within the water droplet, further emulsifying the system. The trapped thin film is also dynamic within the larger droplet, it can be seen to rise upwards towards the thin neck attached to the capillary. This may be due to the organic thin film experiencing repulsive forces from the polar water phase. Figure 47 demonstrates the relationship between electrocoalescence time and overlap distance.

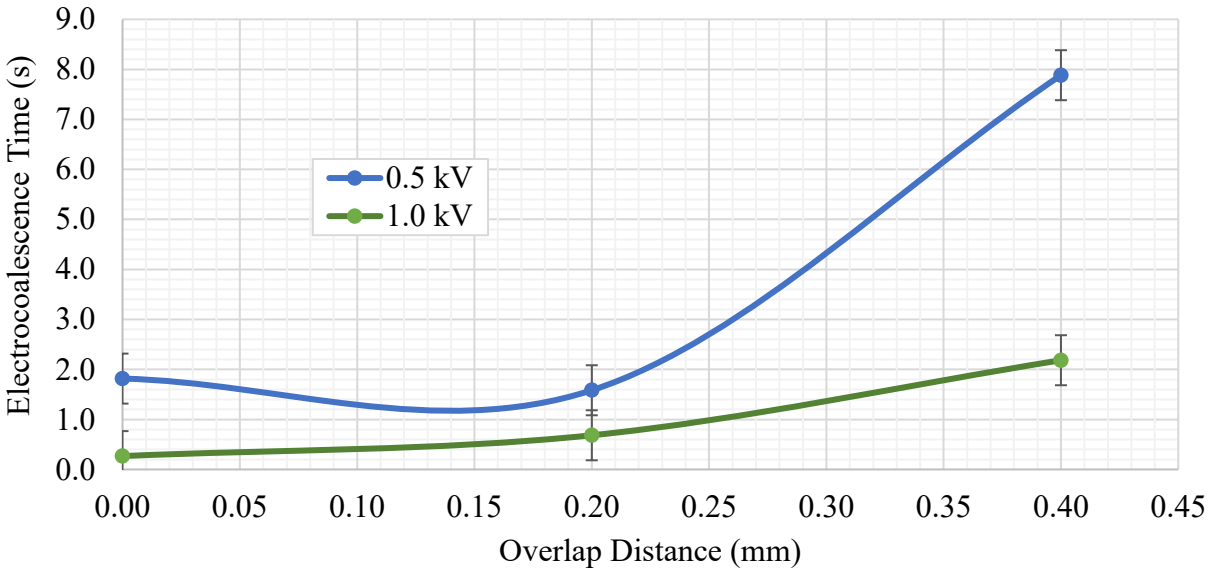

Figure 47. Graph of electrocoalescence time (s) as a function degree of overlap (mm) between droplets in PG/E1.

It is shown here that the greater the degree of droplet overlap, the greater the electrocoalescence time required. This graph confirms that the trapped thin film shown in the images does in fact play a role in slowing down the electrocoalescence process due to the stabilizing methods of reduced surface activity between the droplets. However, at higher electric field strengths,

electrocoalescence may be sped up even with a high degree of overlap, demonstrating that the electric forces are still dominant in this case. Overall, we can state that increasing the droplet overlap distance does work to compress the interfacial fluid in between the two droplets, making it more difficult to displace the layer and hence increasing electrocoalescence time, which can especially be seen at a lower electric field strength.

4.3. Electrocoalescence properties of water droplets in complex model oil emulsion

These next sections utilize the complex model oil emulsion consisting of heptol combined with extracted asphaltenes for the organic phase, and salted water acting as the droplets in the emulsion. As mentioned in Chapter 3 Materials and Methods, it is very difficult to utilize a crude oil as the camera will not pick up the water droplets, so a model crude oil had to be made up. In the previous subchapters, a model oil consisting of a high concentration of Span 80 surfactant resulted in a strong viscoelastic interfacial layer between the droplets, this durability allowed for many variable experiments to be conducted while droplets are in contact. However, when using the complex model emulsion oil, the droplets were required to age in the oil phase for at least 30 minutes in order for the extracted asphaltenes to form a film. Even with this, the interfacial layer remained more delicate, allowing for the droplets to coalesce much easier and at lower electric field strengths. For the following results, experiments were run with leaving a separation distance between the droplets.

4.3.1. Electric field application ramp speed

Electric field application ramp speed experiments were conducted for the simple model emulsion in E2 position, that is, with the droplets already in contact as the electric field strength is ramped up. In the results for complex, asphaltene based model emulsion, using the E2 position with ramp speed resulted in immediate coalescence at lower field strengths of around 100 V or

0.05 kV/cm. Hence, applying the electric field with the aged droplets separated is an alternative method to study the effect of application ramp speed as well as the variation between droplet positions during the coalescence process. Figure 48 includes images of droplets in the complex model emulsion undergoing coalescence in the non-contacting (NC) position.

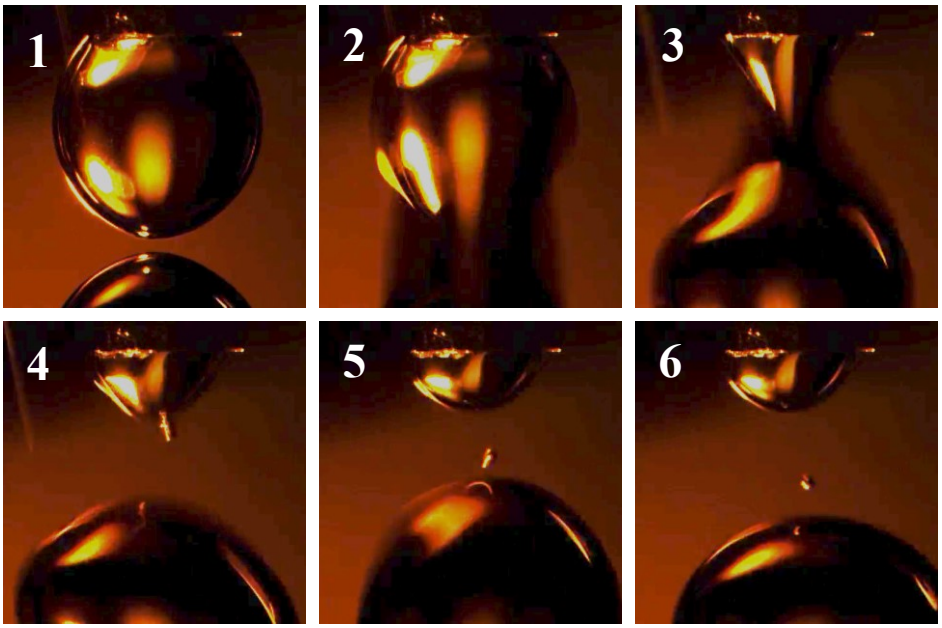

Figure 48. Images of salted water droplets in asphaltene-based oil at 1) NC position, 2) coalescence time (CT), 3) CT + 33 ms, 4) CT + 66 ms, 5-6) secondary droplet formation after coalescence in field range of ~1.25 to 2.25 kV (0.625 to 1.125 kV/cm).

The droplets undergo a similar shape change throughout the electrocoalescence process as compared to the E1 droplet position. The cone shape is formed during coalescence, and a small secondary droplet is formed afterwards. The main difference here is that the upper droplet needs to undergo an attracting force towards the lower droplet as they are separated, unlike the E1 position in which droplets are manually brought into contact using the induction timer software. The graphs below illustrate the relation between the time and field strength needed for droplets to coalesce in the complex model emulsion and E2 position.

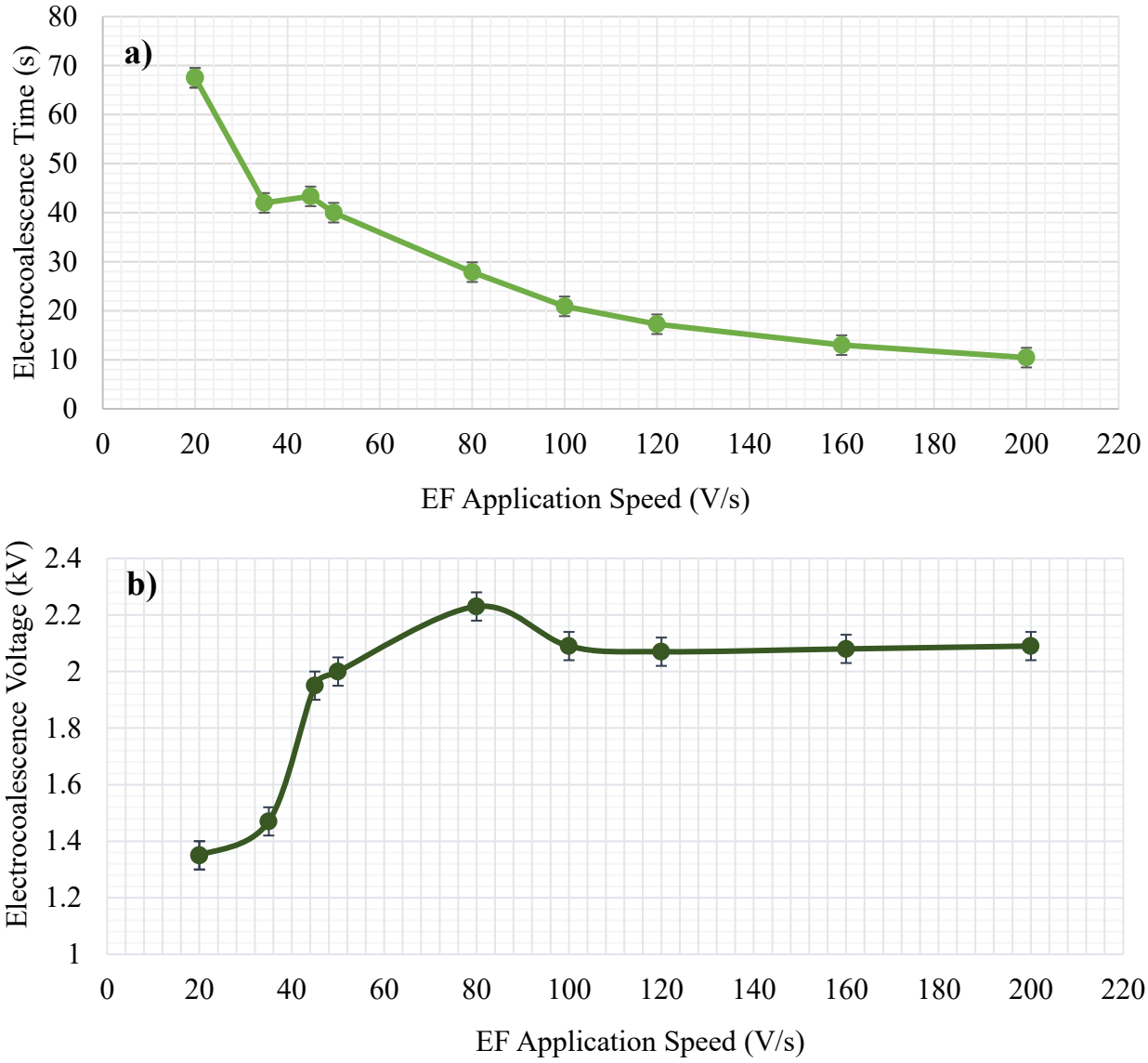

Figure 49. Graphs of a) electrocoalescence time (s) and b) electrocoalescence voltage (kV) as a function of electric field application ramp speed (V/s) in complex model emulsion and PG/NC.

Graph a) shows that the greater the electric field application speed, the faster the electrocoalescence time of the droplets. This is similar to the trend of the simple model emulsion in E2 position, where the time required to coalesce also decreases with increasing the ramp speed. Although the relationship is similar, the overall electrocoalescence time for the NC complex emulsion droplets is at a higher range of around 10 s to 70 s as compared to the range for the E2

simple emulsion droplets of 0.4 s to 16 s. The difference in coalescence time ranges is mainly due to the droplet positions. In the non-contacting position, droplets remain distanced apart, and hence the droplets need to undergo additional attractive forces to be pulled towards each other in order to then undergo coalescence with the assistance of the electric field and surface interactivity. Contacting droplets do not need to undergo as strong of attractive forces as they are separated by a thin interfacial film.

Graph b) indicates that the faster the ramp speed, the higher the voltage required to achieve coalescence. This also has to do with the non-contacting droplet placement as the droplets require more time in order to undergo attractive forces before film draining and surface interactivity can occur. Therefore, the fast ramp speed does not allow much time for the droplets to become attracted at lower field strengths, hence requiring higher voltage ranges of 1.3 kV to 2.2 kV as compared to that of E2 droplets ranging from 0.04 kV to 0.3 kV.

Overall, the trendlines in these graphs reveal an inverse relationship between field application speed and the voltage required for coalescence, as opposed to the same experiment with using simple model oil using E2 droplet positioning. The droplets need to be exposed to the electric field for longer in order to be attracted to each other and coalesce, this is mostly due to the NC droplet placement.

4.3.2. Chemical demulsifiers

Combining chemical demulsifiers with electrocoalescence has rarely been studied and is an up and coming area in surface chemistry research. An effective experimental method was to vary electric field strengths to analyze the effects of chemical demulsifiers on droplet interactions and thin film drainage. This can lead to both qualitative and quantitative results, which may then be translated into useful findings for industry. As there are limited characteristics provided for

industry provided chemical demulsifiers, it is imperative to observe how the addition of these demulsifiers affect the complex model emulsion. NalcoChampion A tends to stabilize the droplets as they are able to be brought into contact after aging in the asphaltene-based oil. Hence, the droplets' interactions can be studied E1 position and can be compared with the simple model emulsion with no demulsifier as shown in Figure 50.

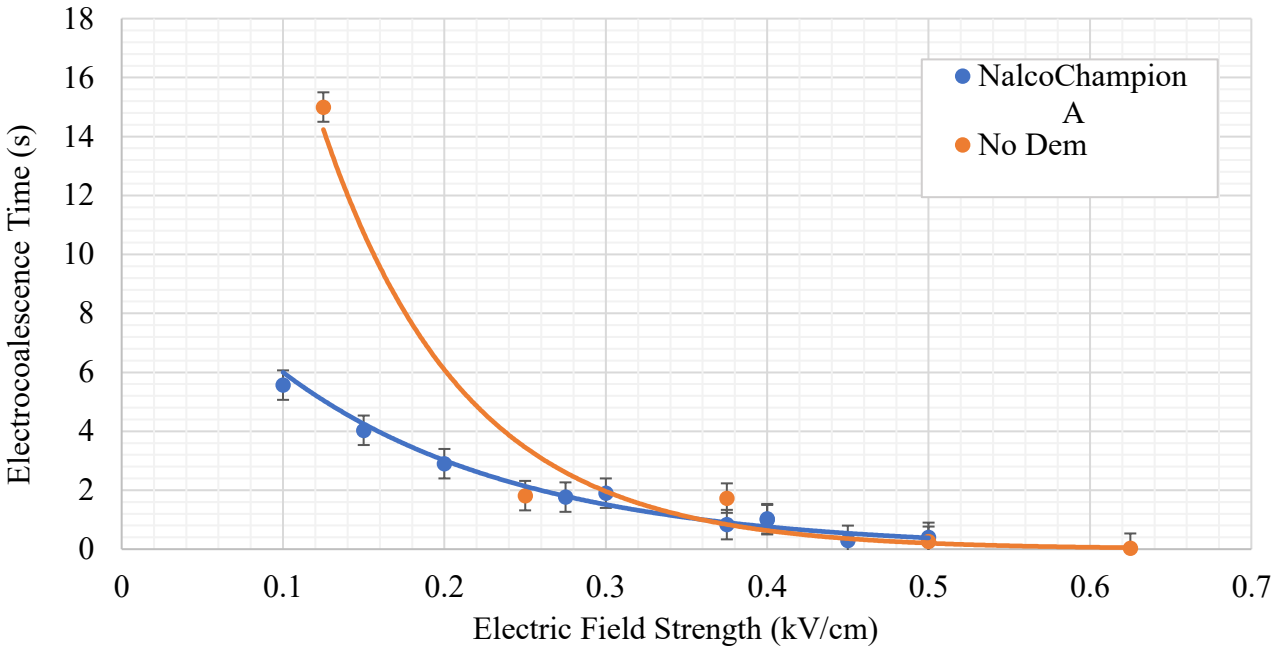

Figure 50. Graph of electrocoalescence time (s) as a function of electric field strength (kV/cm) in PG/E1.

As shown in the graph above, the electrocoalescence time is shorter overall with the addition of the chemical demulsifier, as compared to the original simple model oil with no demulsifier. As stated by Mhatre (2018), the presence of demulsifiers does not explicitly alter the electrostatic force, it determines the capillary and lubrication forces in the film between electrocoalescing droplets. The droplets appear to experience an overall decrease in interfacial tension as studied in our group (by Ye Zhang) when undergoing electric field stresses alone. Hence, the addition of a demulsifier functions to assist in coalescence by destabilizing droplet surface properties through

increasing droplet deformation, which may be due to demulsifiers assisting the decrease in interfacial tension.

Interfacial tension is a main contributor to the stabilization of water droplets in an oil emulsion. The common conception that applies to droplets in the absence of an electric field is that the higher the interfacial tension, the more rigid the droplets, and the more likely they are able to undergo coalescence. This should imply that since an electric field causes droplets to coalesce much faster, that this is due to an increase in interfacial tension. A method used to test this hypothesis was to conduct experiments in our group (provided by Ye Zhang) using a Tensiometer in order to study the effect of electric field application on the interfacial tension of a single droplet. Using a computer software that evaluates shape factor and uses the Young-Laplace equation to numerically determine the interfacial tension returns the following results.

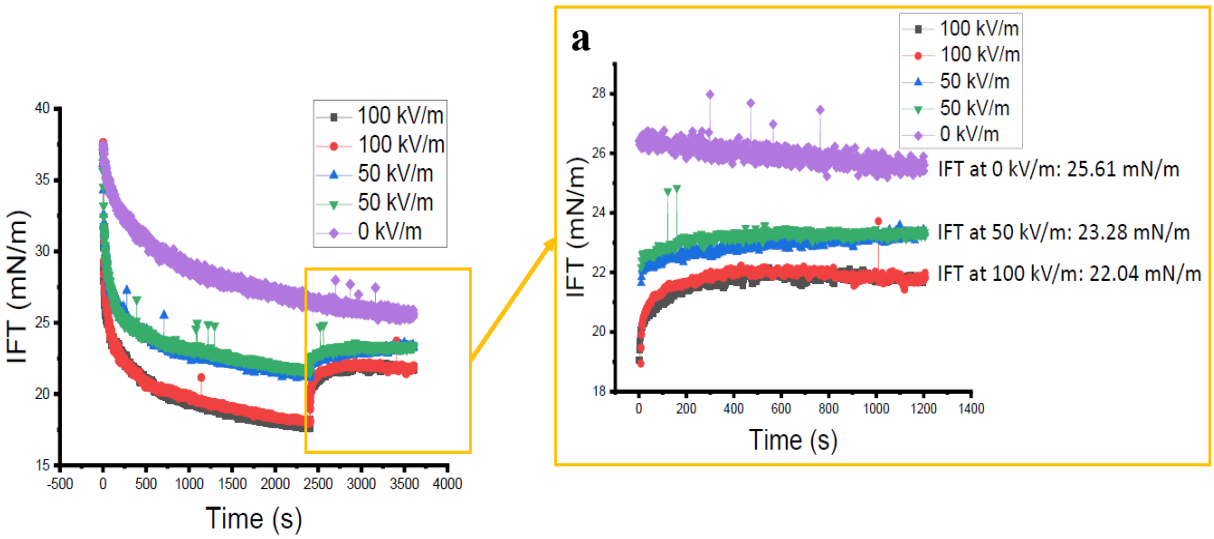

Figure 51. Interfacial tension values of water droplet in oil under electric field with a) plateau of relaxation.

Figure 51 shows the calculated interfacial tension values of a single water droplet in oil solvent undergoing the transition from being under an electric field to turning it off (plateau of relaxation).

The IFT values are measured at various electric field strengths, with the trendlines showing that the interfacial tension of the droplet tends to decrease with the addition of an electric field. This means that the Young-Laplace equation used to determine the IFT requires modification in order to account for the pressure or stress from the electric field. The following equations are derived, showing a possible relationship:

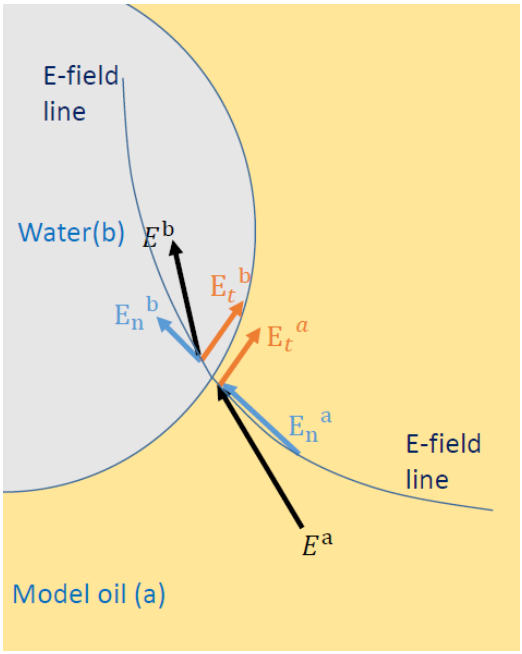

Figure 52. Diagram of single pendant water drop in electric field.

Electrical pressure jump: $\Delta P_e = \frac{1}{2}\left[\epsilon^a \, {E_n}^{a^2} - \epsilon^b \, {E_n}^{b^2} + (\epsilon^b - \epsilon^a){E_t}^2\right]$

Advanced Young-Laplace equation: $\gamma\left(\frac{1}{R_1} + \frac{1}{R_2}\right) = \Delta P_0 + (\Delta\rho)gz + \Delta P_e$

Two conclusions can be made from these observations; first, the Young-Laplace equation is not accurate enough on its own in order to predict the IFT from the Tensiometer's reading of shape factor due to the significant pressure and force from the electric field application and Maxwell stress. Second, the assistance of electrocoalescence is not achieved by weakening the formation of asphaltene skin or displacing it, the droplets themselves are acted on. These data trends are agreeable with research claims which states that under applied electric fields, lowering interfacial

tension facilitates aqueous-drop coalescence in the organic phase due to the deformation and elongation of the droplets; they more readily undergoing the Coloumbic force and electric Maxwell stresses that promote drop contact and coalescence.

More measurements are required to be analyzed, including varying demulsifier concentration; the concentration used in Figure 53 is around 0.25% vol. which is above the recommended amount determined by joint industry research partners. The graph below in shows trends of critical electric field strengths as a function of concentrations of various demulsifiers.

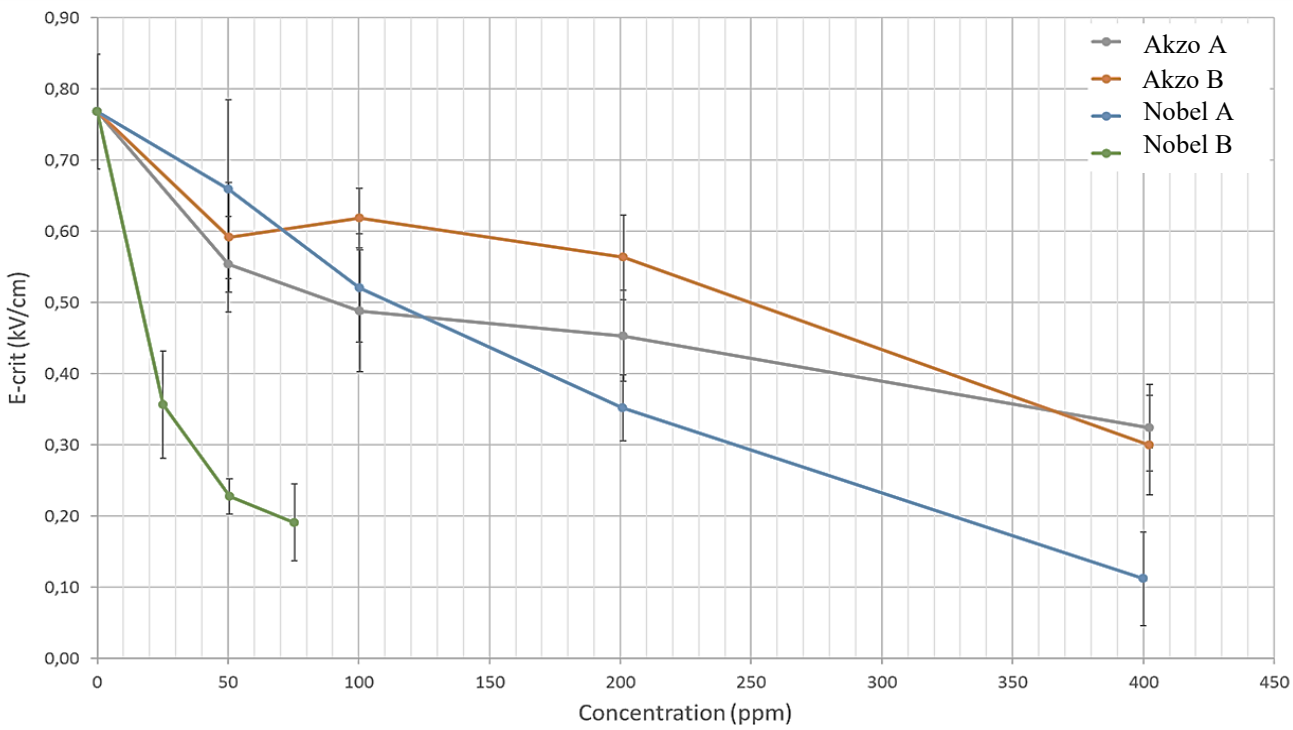

Figure 53. Graph of E-crit (kV/cm) as a function of chemical demulsifier concentration (ppm) at 25°C for a single crude oil emulsion droplet of 50% water cut.

These trends show that the strength of electric field required to burst a droplet (E_c: critical electric strength) decreases with increasing demulsifier concentration. Hence, the strength of an electric field needed to induce coalescence is an overall lower voltage due to the droplet's behavior when combined with a demulsifier. Finding a demulsifier concentration in which E_c can be reached

and optimal electrocoalescence rate may occur will be of major importance to dewatering W/O emulsions.

4.4. Notable phenomena

This subchapter includes some phenomena observed within the simple model emulsion systems in an applied electric field.

4.4.1. Secondary droplet formation

Secondary droplets may be formed by partial coalescence, this leads to decreased separation efficiency due to the smaller droplet sizes. It has been observed that the higher the electric field strength used, the more likely that partial coalescence will be favored over full coalescence [61]. The necking process, observed in the figure below, is present in non-electric coalescence processes, to a lesser extent.

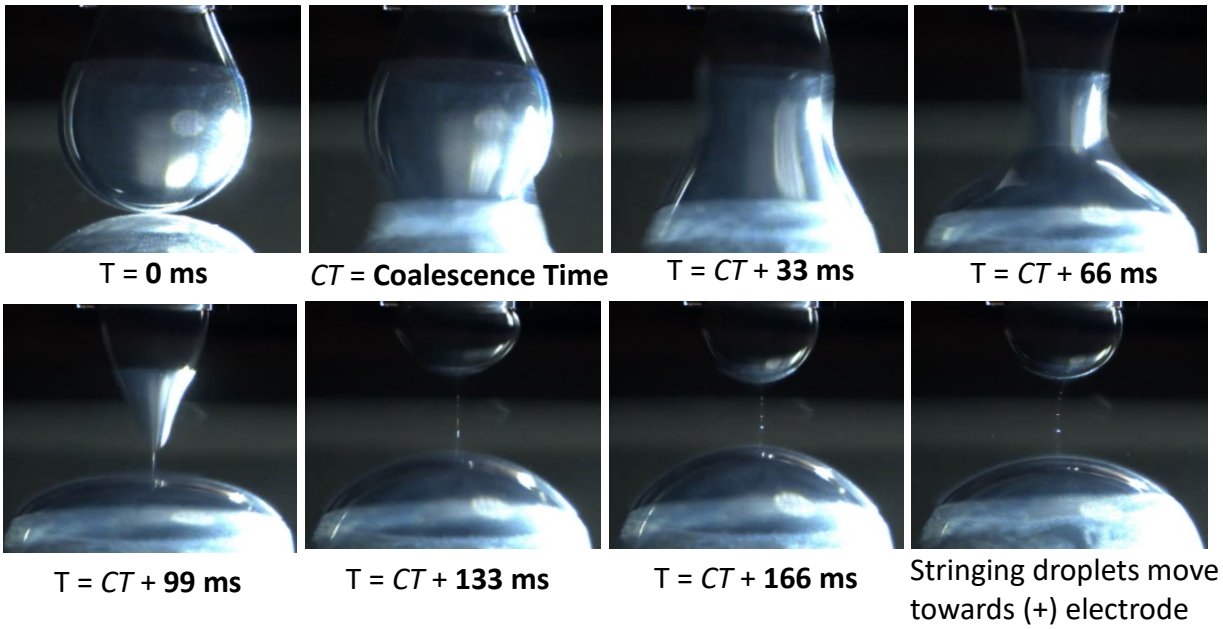

Figure 54. Frame-by-frame breakdown of electrocoalescence process of water-in-oil droplets, resulting in string chain.

Figure 54 shows one type of partial coalescence outcome that is undesirable as it results in smaller water droplets that may be even more difficult to coalesce in the future. String chains usually result after faster coalescence time interactions and at higher electric field strengths, as suggested by Mousavichoubeh et al.

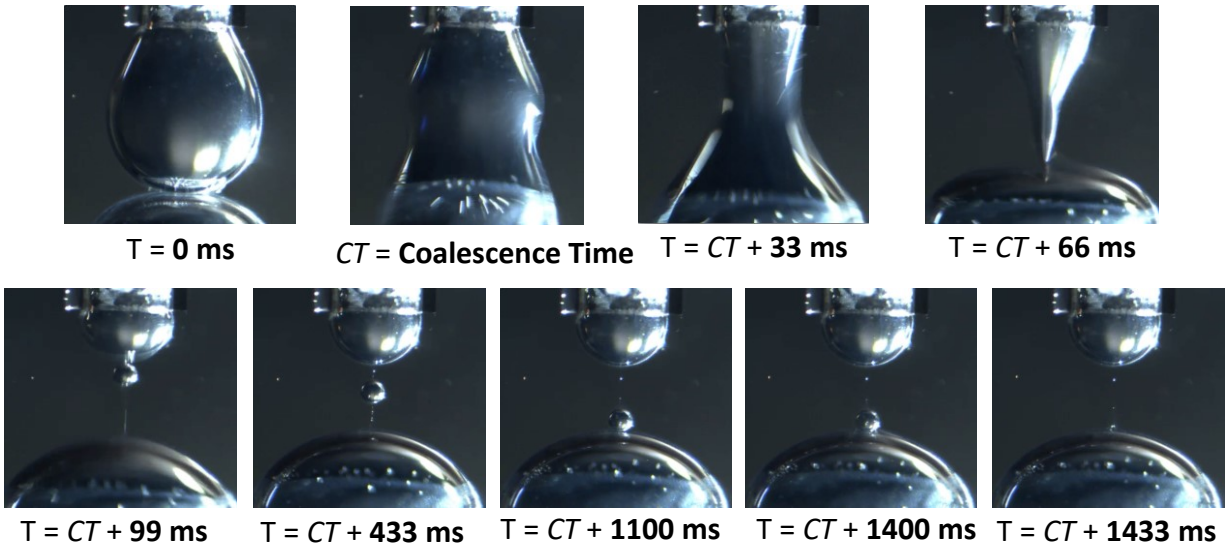

Figure 55. Frame-by-frame breakdown of electrocoalescence process of water-in-oil droplets, resulting in small droplet.

This type of partial coalescence is also observed, where a small droplet is formed rather than a string chain of droplets. This typically occurs when coalescence time is slower and at lower electric field strengths. In the last frame, we can see that the small droplet re-coalesces with the larger "coalesced" droplet due to the electric field still being applied and the vicinity of the droplets.

4.4.2. Dipole alternating bouncing droplet

An interesting observation occurs with non-stationary (or free floating) water droplets in the surfactant-based model oil. Water droplets initially resting on the surface of the ground electrode begin to experience a pull upwards toward the positive electrode when the electric field is turned on. Once the electric field strength nears the system's critical electric field strength, the droplet

experiences a strong attractive force to the positive electrode and moves in an upward motion towards it. As soon as the drop contacts the positive electrode, it almost simultaneously experiences a repulsive force, causing the droplet to quickly shoot back downwards towards the ground electrode. Once in contact with the ground electrode, the droplet is repelled and is once again attracted to the positive electrode; this process continues to repeat.

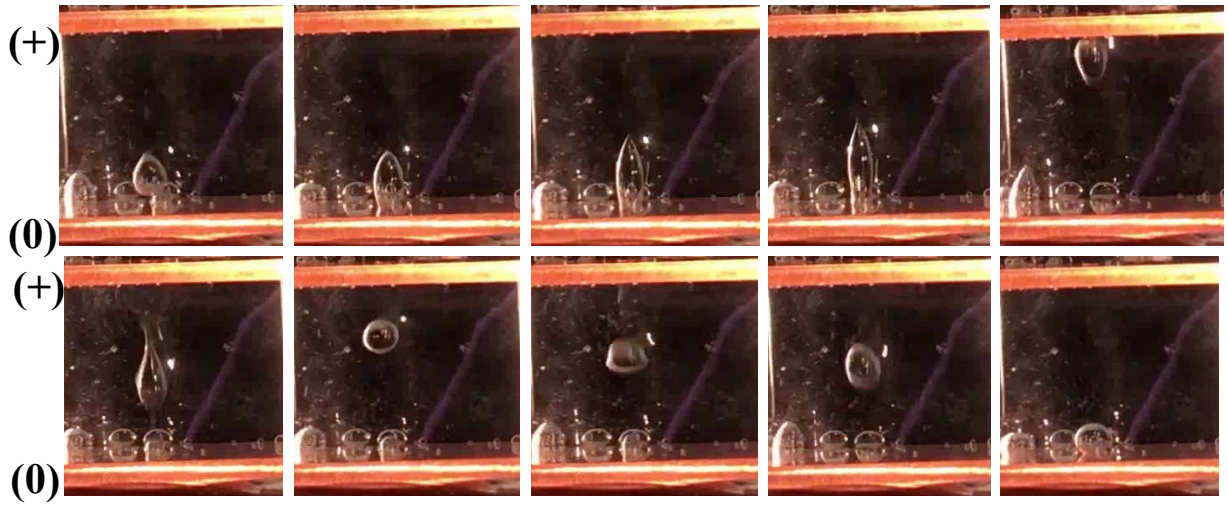

Figure 56. "Bouncing" water droplet under electric field.

This phenomenon is commonly observed and appears to be driven charge transfer dynamics. The electric field remains constant, nearing the E_c, with the droplet travelling upwards against gravity due to the electrostatic force from the positive electrode. The reversal of direction following each bounce is due to the net charge in the drop alternating charge signs, which means charge must be transmitted through the electrode or droplet during the bounce [62].

Chapter 5 Conclusions and Future Work

5.1. Conclusions

A multitude of techniques can be combined and utilized in order to result in more efficient and effective demulsification of water droplets in oil emulsions. It is evident that the electrical, physical, and chemical components all play crucial roles in droplet surface activity, some variables having more impact than others. Electrical variables explored included electric field application strength, time, direction, and speed. The strength of the electric field proved to be a crucial variable in order to set the correct range of voltage to be used in experimentation, with the critical field strength found to be around 3 kV (or 1.5 kV/cm). While the direction of the electrode charge or field acting on the droplets (parallel vs. perpendicular) did not show significantly varied results, it is preferable to use the parallel electric field setup with a gravity-directed movement. The electric field application speed applied to the system greatly impacts the coalescence rate of droplets, where faster electric fields resulted in faster overall electrocoalescence times, but the voltage at which droplets coalesced was shown to vary with droplet positioning. Droplets positioned separate from one another (NC position) generally required more time to coalesce due to the addition of attractive forces required for the droplets to overcome the greater separation distance, as compared to droplets already in contact (E1 and E2 positions).

Physical variables studied include varying droplet size and overlap distance. We can conclude that the greater the droplet radii, the more time required for droplets to coalesce due to several factors that include droplet instability and a larger surface area that requires more time for the droplet interaction. Smaller droplets that have smaller surface areas which trap less interfacial film and are more surface active, allowing for faster coalescence. We can also state that increasing the droplet overlap distance does work to compress the interfacial fluid in between the two

droplets, displacing the interfacial layer becomes more difficult and increases electrocoalescence time. Chemical variables including modifying surfactant concentration and chemical demulsifiers were researched. As expected, electrocoalescence time is delayed with increasing surfactant concentration, and is increased with the addition of a chemical demulsifier up to a certain concentration.

Interfacial tension is shown to decrease under electric field stresses which elongates the droplets, favoring interaction and electrocoalescence. Coulombic attractive forces between the droplets and Maxwell force from the electric field trigger electrocoalescence. Secondary drop formation and the "bouncing ball" droplet phenomena are also demonstrated.

5.2. Future work

The field of electrocoalescence is a topic that is currently being explored; however, there are many gaps that may be filled through experimentation and modelling. For future work in this research project, it is necessary to conduct further experiments in areas including using chemical demulsifiers in combination with some key variables, as well as looking into surface force apparatus methods. An experimental modification could also include multi-droplet emulsions using non-stationary droplets, as well as introducing variation in emulsion temperature and the ionic strength of the water phases as other research in literature prove these are also key variables that impact droplet behavior and coalescence rates.

References

[1] B. B. Wang, X. D. Wang, T. H. Wang, G. Lu, and W. M. Yan, "Electro-coalescence of two charged droplets under constant and pulsed DC electric fields," *Int. J. Heat Mass Transf.*, vol. 98, pp. 10–16, 2016.

[2] P. Tchoukov, F. Yang, Z. Xu, T. Dabros, J. Czarnecki, and J. Sjöblom, "Role of asphaltenes in stabilizing thin liquid emulsion films," *Langmuir*, vol. 30, no. 11, pp. 3024–3033, 2014.

[3] J. H. Masliyah, J. Czarnecki, and Z. Xu, "Handbook on theory and practice of bitumen recovery from Athabasca oil sands - Volume 1: Theoretical basis," *Kingsley Knowl. Publ.*, pp. 115–116, 2011.

[4] K. B. Mhatre S, Vivacqua V, Ghadiri M, Abdullah A, Al-Marri M, Hassanpour A, Hewakandamby B, Azzopardi B, "Electrostatic phase separation: A review," *Chem. Eng. Res. Des.*, vol. 96, pp. 177–195, 2015.

[5] A. G. Bailey and E. Borzabadi, "Natural periodic electrostatic spraying of liquids," *IEEE Trans. Ind. Appl.*, no. 2, pp. 162–167, 1978.

[6] C. Tsouris, D. W. DePaoli, J. Q. Feng, and T. C. Scott, "Experimental investigation of electrostatic dispersion of nonconductive fluids into conductive fluids," *Ind. Eng. Chem. Res.*, vol. 34, no. 4, pp. 1394–1403, 1995.

[7] C. Tsouris, W.-T. Shin, S. Yiacoumi, and D. W. DePaoli, "Electrohydrodynamic velocity and pumping measurements in water and alcohols," *J. Colloid Interface Sci.*, vol. 229, no. 2, pp. 335–345, 2000.

[8] J. Sjöblom, O. Urdahl, H. Høiland, A. A. Christy, and E. J. Johansen, “Water-in-crude oil emulsions. Formation, characterization, and destabilization,” in *Surfactants and Macromolecules: Self-Assembly at Interfaces and in Bulk*, Springer, 1990, pp. 131–139.

[9] J. Klier, “Microemulsions,” in *Kirk-Othmer Encyclopedia of Chemical Technology*, American Cancer Society, 2012, pp. 1–22.

[10] J. Sjoblom, *Encyclopedic handbook of emulsion technology*. CRC Press, 2001.

[11] T. S. Horozov and B. P. Binks, “Particle-stabilized emulsions: A bilayer or a bridging monolayer?,” *Angew. Chemie - Int. Ed.*, vol. 45, no. 5, pp. 773–776, 2006.

[12] J. S. Eow, M. Ghadiri, A. O. Sharif, and T. J. Williams, “Electrostatic enhancement of coalescence of water droplets in oil: A review of the current understanding,” *Chem. Eng. J.*, vol. 84, no. 3, pp. 173–192, 2001.

[13] C. Lesaint, W. R. Glomm, L. E. Lundgaard, and J. Sjöblom, “Dehydration efficiency of AC electrical fields on water-in-model-oil emulsions,” *Colloids Surfaces A Physicochem. Eng. Asp.*, vol. 352, no. 1–3, pp. 63–69, 2009.

[14] M. Fortuny, C. B. Z. Oliveira, R. L. F. V. Melo, M. Nele, R. C. C. Coutinho, and A. F. Santos, “Effect of salinity, temperature, water content, and pH on the microwave demulsification of crude oil emulsions,” *Energy & Fuels*, vol. 21, no. 3, pp. 1358–1364, 2007.

[15] M. Hosseini, “Coalescence behaviour of water droplets in water oil interface under pulsatile electric fields,” *Chinese J. Chem. Eng.*, vol. 24, no. 9, pp. 1147–1153, 2016.

[16] Y. Zhang, Y. Liu, X. Wang, Z. Li, and Y. Shen, “Simulation of droplet behavior in water-

in-oil emulsion subjected to an electric field," *J. Dispers. Sci. Technol.*, vol. 36, no. 2, pp. 259–267, 2015.

[17] A. Srivastava, S. Karthick, K. S. Jayaprakash, and A. K. Sen, "Droplet demulsification using ultralow voltage-based electrocoalescence," *Langmuir*, vol. 34, no. 4, pp. 1520–1527, 2018.

[18] B. P. Binks, "Particles as surfactants: Similarities and differences," *Curr. Opin. Colloid Interface Sci.*, no. 7, pp. 21–41, 2002.

[19] D. E. Tambe and M. M. Shaftma, "The effect of colloidal particles on fluid-fluid interfacial properties and emulsion stability," *Adv. Colloid Interface Sci.*, vol. 52, pp. 1–62, 1994.

[20] S. L. Kokal, "Crude oil emulsions: A state-of-the-art review," *Soc. Pet. Eng.*, vol. 20, no. 1, pp. 5–13, 2005.

[21] F. Opawale and D. Burgess, "Influence of interfacial properties of lipophilic surfactants on water-in-oil emulsion stability," *J. Colloid Interface Sci.*, vol. 197, no. 1, pp. 142–50, 1998.

[22] P.-G. de Gennes, F. Brochard-Wyart, and D. Quéré, "Capillarity and wetting phenemona: drops, bubbles, pearls, and waves," p. 292, 2004.

[23] L. S. C. Wan and P. F. S. Lee, "Studies on surface films of sorbitan-esters at air/water interface," *Can. J. Pharm. Sci.*, vol. 9, no. 3, pp. 82–85, 1974.

[24] J. Sjoblom, *Emulsions and emulsion stability: Surfactant science series*, Second edi. CRC Press, 2005.

[25] D. Myers, *Surfactant science and technology*. John Wiley & Sons, 2005.

[26] P. Becher and W. A. Hamor, *Emulsions: Theory and practice*, vol. 135. Reinhold New York, 1957.

[27] Y. Kawashima, T. Hinoo, H. Takeuchi, and T. Niwa, "Stabilization of water/oil/water multiple emulsion with hypertonic inner aqueous phase," *Chem. Pharm. Bull.*, vol. 40, no. 5, pp. 1240–1246, 1992.

[28] Sigma-Aldrich, "Span 80 surfactant," 2018. [Online]. Available: https://www.sigmaaldrich.com/catalog/product/sigma/s6760?lang=en&region=CA.

[29] N. I. Politova, S. Tcholakova, S. Tsibranska, N. D. Denkov, and K. Muelheims, "Coalescence stability of water-in-oil drops: Effects of drop size and surfactant concentration," *Colloids Surfaces A Physicochem. Eng. Asp.*, vol. 531, no. June, pp. 32–39, 2017.

[30] Z. Liu, S. T. Chan, H. A. Faizi, R. C. Roberts, and H. C. Shum, "Droplet-based electro-coalescence for probing threshold disjoining pressure," *Lab Chip*, vol. 15, no. 9, pp. 2018–2024, 2015.

[31] A. Sharma and O. C. Mullins, "Insights into molecular and aggregate structures of asphaltenes using HRTEM," in *Asphaltenes, heavy oils, and petroleomics*, Springer, 2007, pp. 205–229.

[32] H. W. Yarranton, H. Alboudwarej, and R. Jakher, "Investigation of asphaltene association with vapor pressure osmometry and interfacial tension measurements," *Ind. Eng. Chem. Res.*, vol. 39, no. 8, pp. 2916–2924, 2000.

[33] O. P. Strausz, T. W. Mojelsky, and E. M. Lown, “The molecular structure of asphaltene: an unfolding story,” *Fuel*, vol. 71, no. 12, pp. 1355–1363, 1992.

[34] H. Groenzin and O. C. Mullins, “Molecular size and structure of asphaltenes from various sources,” *Energy and Fuels*, vol. 14, no. 3, pp. 677–684, 2000.

[35] X. Luo, H. Yin, H. Yan, X. Huang, D. Yang, and L. He, “The electrocoalescence behavior of surfactant-laden droplet pairs in oil under a DC electric field,” *Chem. Eng. Sci.*, vol. 191, pp. 350–357, 2018.

[36] D. Sun, S. C. Jong, X. D. Duan, and D. Zhou, “Demulsification of water-in-oil emulsion by wetting coalescence materials in stirred- and packed-columns,” *Colloids Surf. A*, vol. 150, no. 1–3, pp. 69–75, 1999.

[37] J. Dong, V. F. de Almeida, and C. Tsouris, “Effects of applied electric fields on drop—interface and drop—drop coalescence,” *J. Dispers. Sci. Technol.*, vol. 23, no. 1–3, pp. 155–166, 2002.

[38] P. Atten, “Electrocoalescence of water droplets in an insulating liquid,” *J. Electrostat.*, vol. 30, pp. 259–270, 1993.

[39] S. Mhatre, “Dielectrophoretic motion and deformation of a liquid drop in an axisymmetric non-uniform AC electric field,” *Sensors Actuators, B Chem.*, vol. 239, pp. 1098–1108, 2017.

[40] S. Mhatre and R. Thaokar, “Electrocoalescence in non-uniform electric fields: An experimental study,” *Chem. Eng. Process. Process Intensif.*, vol. 96, pp. 28–38, 2015.

[41] G. Roussy and J. A. Pearce, “Foundations and industrial applications of microwaves and

radio frequency fields. Physical and chemical processes.," in *Proceedings of the 6th International Conference on Optimization of Electrical and Electronic Equipments*, 1998, vol. 1, pp. 115–116.

[42] J. Hempoonsert, B. Tansel, and S. Laha, "Effect of temperature and pH on droplet aggregation and phase separation characteristics of flocs formed in oil--water emulsions after coagulation," *Colloids Surfaces A Physicochem. Eng. Asp.*, vol. 353, no. 1, pp. 37–42, 2010.

[43] C. Guo, L. He, and Y. Xin, "Coalescence behavior of two water drops in viscous oil under an AC electric field," *Pet. Sci. Technol.*, vol. 72, no. 6, pp. 470–476, 2014.

[44] G. Berg, L. E. Lundgaard, and N. Abi-Chebel, "Electrically stressed water drops in oil," *Chem. Eng. Process. Process Intensif.*, vol. 49, no. 12, pp. 1229–1240, 2010.

[45] S. Mhatre, S. D. Deshmukh, and R. M. Thaokar, "Stability of a charged drop near a conductor wall," *Eur. Phys. J. E*, vol. 35, no. 5, 2012.

[46] B. B. Wang, X. D. Wang, T. H. Wang, and W. M. Yan, "Electrocoalescence behavior of two identical droplets with various droplet radii," *Appl. Therm. Eng.*, vol. 111, pp. 1464–1469, 2017.

[47] J. S. Eow, M. Ghadiri, and A. Sharif, "Experimental studies of deformation and break-up of aqueous drops in high electric fields," *Colloids Surfaces A Physicochem. Eng. Asp.*, vol. 225, no. 1–3, pp. 193–210, 2003.

[48] J. Wu, Y. Xu, T. Dabros, and H. Hamza, "Effect of demulsifier properties on destabilization of water-in-oil emulsion," *Energy and Fuels*, vol. 17, no. 6, pp. 1554–

1559, 2003.

[49] S. Mhatre, S. Simon, J. Sjöblom, and Z. Xu, “Demulsifier assisted film thinning and coalescence in crude oil emulsions under DC electric fields,” *Chem. Eng. Res. Des.*, vol. 134, pp. 117–129, 2018.

[50] L. Y. Zhang, Z. Xu, and J. H. Masliyah, “Langmuir and Langmuir-Blodgett films of mixed asphaltene and a demulsifier,” *Langmuir*, vol. 19, no. 23, pp. 9730–9741, 2003.

[51] S. Mhatre, S. Deshmukh, and R. M. Thaokar, “Electrocoalescence of a drop pair,” *Phys. Fluids*, vol. 27, no. 9, 2015.

[52] J. Sjoblom *et al.*, “Modern characterization techniques for crude oils, their emulsions, and functionalized surfaces,” *Surfactant Sci. Ser.*, vol. 132, pp. 415–476, 2006.

[53] S. Less, A. Hannisdal, E. Bjørklund, and J. Sjöblom, “Electrostatic destabilization of water-in-crude oil emulsions: Application to a real case and evaluation of the Aibel VIEC technology,” *Fuel*, vol. 87, no. 12, pp. 2572–2581, 2008.

[54] J. Bi *et al.*, “Interfacial layer properties of a polyaromatic compound and its role in stabilizing water-in-oil emulsions,” *Langmuir*, vol. 31, no. 38, pp. 10382–10391, 2015.

[55] A. Sheludko, “Thin liquid films,” *Adv. Colloid Interface Sci.*, vol. 1, no. 4, pp. 391–464, 1967.

[56] R. H. Davis, J. A. Schonberg, and J. M. Rallison, “The lubrication force between two viscous drops,” *Phys. Fluids A Fluid Dyn.*, vol. 1, no. 1, pp. 77–81, 1989.

[57] P. Atten, “Electrocoalescence of water droplets in an insulating liquid,” *J. Electrostat.*, vol. 30, no. C, pp. 259–269, 1993.

[58] G. Taylor, “Disintegration of water drops in an electric field,” *Proc. R. Soc. A Math. Phys. Eng. Sci.*, vol. 280, no. 1382, pp. 383–397, 1964.

[59] Spellman High Voltage Electronics, “Instruction manual sl series high voltage power supply,” vol. 81. pp. 4–7, 2004.

[60] National Instruments, “Complete guide to building a measurement system: how to choose the right sensor for your measurement system,” 2018.

[61] M. Mousavichoubeh, M. Shariaty-Niassar, and M. Ghadiri, “The effect of interfacial tension on secondary drop formation in electro-coalescence of water droplets in oil,” *Chem. Eng. Sci.*, vol. 66, no. 21, pp. 5330–5337, 2011.

[62] W. D. Ristenpart, J. C. Bird, A. Belmonte, F. Dollar, and H. A. Stone, “Non-coalescence of oppositely charged drops,” *Nature*, vol. 461, no. 7262, pp. 377–380, 2009.